Plume Dynamics and Concentration Fluctuations in Gas Emissions

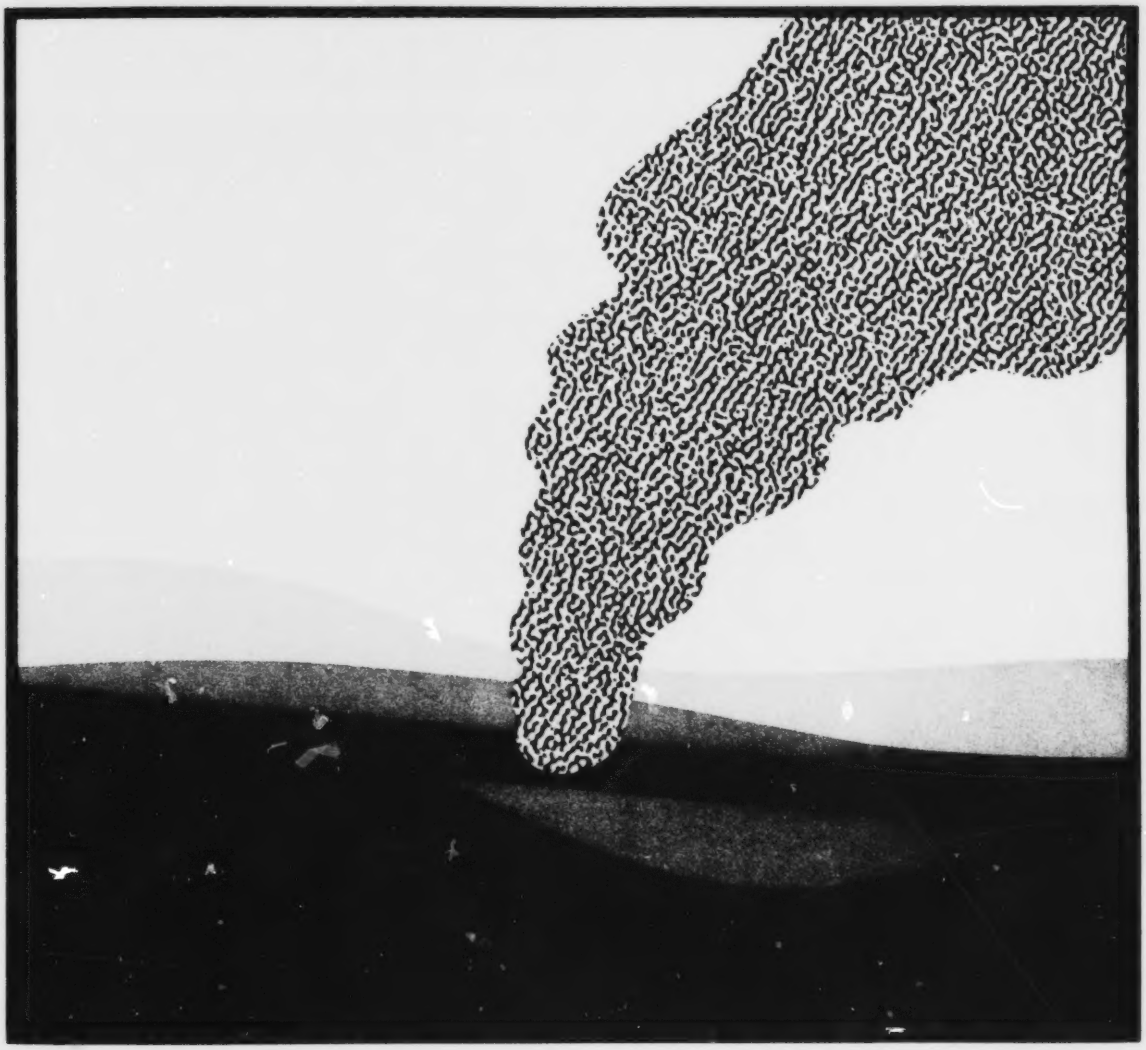

Alberta

ENVIRONMENT

87-01015/

PLUME DYNAMICS AND CONCENTRATION FLUCTUATIONS IN GAS EMISSIONS

By

D.J. Wilson
Department of Mechanical Engineering
University of Alberta
Edmonton, Alberta, Canada

prepared for

ALBERTA ENVIRONMENT
9820 - 106 Street
Edmonton, Alberta T5K 2J6

Project Officer: R.P. Angle
Air Quality Control Branch
Pollution Control Division
Environmental Protection Services

Contract No. 840702

April 1986

TABLE OF CONTENTS

	Page
Acknowledgements	ii
Nomenclature	iii
Executive Summary	viii
CHAPTER 1 - Introduction	1
CHAPTER 2 - Dispersion From Transient Releases	3
Limiting Cases: Puffs and Steady Plumes	3
Transition From Puff-like to Plume-like Dispersion	5
Characteristic Release Duration	8
Estimating Along-Wind Spread	9
Estimating Instantaneous Plume or Puff Spread	10
Experimental Verification of Instantaneous Spread Predictions	13
Summary	18
CHAPTER 3 - Source Size Effects on Concentration Fluctuations	19
Along-Wind Variation of Fluctuation Intensity	20
Source Size Effects Derived from Turbulence	22
Accounting for Wind Shear and Inhomogeneous Turbulence	24
Surface Effects on Variance Profiles	29
Intensity of Conditionally Averaged Fluctuations	31
Effective Source Size for a Vertical Jet	32
Summary	35
CHAPTER 4 - Dilution Caused by Self-Generated Plume Turbulence	36
Dilution by Self-Generated Turbulence in the Exhaust Jet	36
Dilution Factors for Contaminant Concentrations	39
Transition from Vertical Jet to Bent-Over Plume Behavior	40
Combined Dilution from Self-Generated and Atmospheric Turbulence	42
CHAPTER 5 - Momentum and Buoyancy Contributions to Final Plume Rise	45
Factors Determining Final Plume Rise	46
Plume Breakup Criteria From Local Spectral Scaling	47
Sum of Cubes Approximation to Final Rise	51
APPENDIX A - Total and Instantaneous Plume Spread Determined Directly From Turbulence Parameters	55
Total Plume Spread σ_y	55
Power Law Approximation	57
Instantaneous Plume Width	58
Estimates of Instantaneous Spread	59
Spectral Bandpass Model for Relative Diffusion	61

Table of Contents (cont'd)

	Page
Effective Eddy Diffusivity for σ_{iy}	63
Instantaneous Plume Spread Outside the Inertial Subrange	66
APPENDIX B - Along-Wind Development of Concentration Fluctuations	69
Modelling the Dissipation Time Scale T_ε	71
Effective Turbulence Scale Λ in Shear Flows	75
Intensity of Conditionally Averaged Fluctuations	75
APPENDIX C - Entrainment and Dilution by Self Generated Turbulence	77
Dilution in the Source Jet	77
Dilution in a Rising Bent-Over Plume	79
High Pressure Pipeline Ruptures	81
Dilution Factors for Mass and Volume Concentration	83
Transition from Vertical Jet to Bent-Over Plume	85
APPENDIX D - Sum of Cubes Approximation to Final Rise	87
Final Rise Using Briggs Criteria	88
Final Rise of Pure Buoyant Plumes and Momentum Jets	90
Variation of Atmospheric Dissipation with Height	91
Normalizing Plume Rise Variables to Obtain Parametric Solutions	92
Ratio of Combined Final Rise to "Sum of Cubes of Final Rises" Approximation	94
REFERENCES	97

List of Figures

Fig. 2-1 Along-wind diffusion at the nose and tail of a transient suddenly started and stopped plume.

Fig. 2-2 Instantaneous σ_{iy} (triangles) and time-averaged σ_y (circles) spread of a plume from a d = 0.7 cm source in grid turbulence. Data from Nappo (1984). Theory from (2-15), (2-16) and (2-18), (2-19) with $A_1 = 1.0$, $v'/U_c = 0.062$ $\Lambda_v = 17$ cm

Fig. 2-3 Ratio of instantaneous to total, time averaged, plume spread variances in grid turbulence experiments of Nappo (1984). Theory from (2-15), (2-16) and (2-18), (2-19). Hanna's theory from (2-20); $\sigma_s = 0.7$ cm, $A_1 = 1.0, v'/U_c = 0.062$, $\Lambda_v = 17$ cm

Fig. 3-1 Inertial subrange theory for intermittency and total concentration fluctuation intensity for an elevated source at h/H = 0.192 in a wind tunnel boundary layer of H = 120 cm. Data of Fackrell and Robins (1982a) theory from (3-10), (3-11), (3-12) and (3-13), (3-14), (3-15) with $\alpha = 0.6$, $\phi_z = 0.706$

Fig. 3-2 Semi-empirical theory for intermittency and total concentration fluctuation intensity for an elevated source at h/H = 0.192 in a wind tunnel boundary layer of H = 120 cm. Data of Fackrell and Robins (1982a), theory from (3-1), (3-2) and (3-13), (3-14) and (3-15) with $\alpha = 0.6$, $\phi_z = 0.706$.

Fig. 3-3 Inertial subrange theory for along-wind variation of conditional concentration fluctuation intensity on plume axis for an elevated source in a wind tunnel boundary layer. Data from Wilson, Robins and Fackrell (1985). Theory from (3-19), (3-20) and (3-13), (3-14), (3-15) with $\alpha = 0.6$ and $\phi_z = 0.706$

Fig. 3-4 Semi-empirical theory for along-wind variation of conditional concentration fluctuation intensity on plume axis for an elevated source in a wind tunnel boundary layer, from Wilson, Robins and Fackrell (1985). Theory from (3-18) and (3-13), (3-14), (3-15) with $\alpha = 0.6$, $\phi_z = 0.706$

Fig. 4-1 Expansion and entrainment into a bent-over buoyant jet from a high pressure pipe release

Fig. 5-1 Error induced by using sum of cubes law for separate momentum and buoyant final rises instead of combined final rise. Theory from (D25), (D35) and (D28), (D36).

ACKNOWLEDGEMENTS

The theoretical models for plume dispersion and concentration fluctuations were developed with the aid of research grants from the Natural Sciences and Engineering Research Council of Canada, and from Imperial Oil Ltd. Several drafts of the text were typed by Gail Anderson, and the figures were drawn by Marlene Wilson.

NOMENCLATURE

a	exponent for along-wind variation of concentration fluctuation intensity, see (3-4)
a_y	crosswind spread exponent, see (A2)
A	gas molecular weight
C	time or ensemble averaged mean volume fraction, m^3/m^3
$\bar{c}$	time or ensemble averaged mean mass concentration, kg/m^3
$\overline{c'^2}$	concentration fluctuation variance, kg^2/m^6
d_{eff}	effective isokinetic source diameter of a vertically directed jet, see 3-21, m
d_s	"source" diameter of a jet after expansion from a high pressure release, see (3-22), m
d	source diameter for isokinetic injection in the x direction
D_y	crosswind spread constant, see (A2) and (A8)
f	mass fraction of pollutant, kg/kg
F	buoyancy flux, see (D4), m^4/s^3
F_M	momentum flux, see (D3), m^4/s^2
h	$(h_s + \Delta h)$ source height above ground, m
H	thickness of the lower portion of the atmospheric boundary layer that is influenced by mechanical turbulence from surface roughness, m
Δh	plume rise, m
Δh_B	buoyancy rise of a plume at a specified downwind distance, m
Δh_{Bf}	buoyancy-induced component of final plume rise, m
$\Delta \tilde{h}_{Bf}$	final rise of a purely buoyant plume, m
Δh_f	actual final rise of a plume including buoyancy and momentum components, m
$\Delta \tilde{h}_f$	approximate final rise estimated by combining the separate rises of a purely buoyant plume and a pure momentum jet using a sum of cubes law, see (5-12), m

Δh_M momentum rise of a bent-over jet a specified downwind distance, m

$\Delta \tilde{h}_{Mf}$ final rise of a pure momentum jet, m

Δh_{Mf} momentum-induced component of final plume rise, m

h_v effective height of the concentration variance source, see (3-14), m

$\hat{i}$ total RMS concentration fluctuation intensity in homogeneous flow (i.e. in the absence of wind shear or ground surface effects)

i_∞ RMS concentration fluctuation intensity in the absence of the image sources and sinks (which account for dissipation of $\overline{c'^2}$ by wind shear and other ground surface effects), see (3-13)

i_p fluctuation intensities formed by the ratio of conditional RMS and mean values $(\overline{c'^2_p})^{0.5}$ and $\bar{c}_p$ which include only periods when non-zero values of concentration are observed

k 1) wavenumber, proportional to inverse wave length, 2π/wavelength, m^{-1}
2) ratio of constant pressure to constant volume gas specific heats

ℓ_k integral length scale of atmospheric turbulence at wavenumber k, m

ℓ_p integral length scale of self-generated plume turbulence, m

L_v integral Lagrangian length scale of the autocorrelation of crosswind velocity v at a point, m

L_w integral Lagrangian length scale of the autocorrelation of vertical velocity w at a point, m

$\dot{m}$ mass flow rate of pollutant and entrained ambient air through a plume or jet cross section, kg/s

$\dot{m}_e$ total mass flow rate from a source; including pollutant mass flow rate Q and flow rate of other components of gas mixture, kg/s

m_r total mass released from a transient source, kg

n power exponent in windspeed profile, $U \propto z^n$

p_a absolute pressure of the atmosphere, N/m^2

p_e absolute pressure of gas at the pipe exit, N/m^2

Q	steady mass release rate "source strength" of pollutant, kg/s
R	plume or jet radius, m
R_e	radius of pipe exit, see Figure 4-1, m
R_s	radius of the "source" jet after its expansion to atmospheric pressure outside the pipe exit, see Figure 4-1, m
t	time after start of release, s
t_d	weighted release duration, see (2-6), s
t_f	travel time to actual final rise, s
$\tilde{t}_{Bf}$	travel time to final rise of a purely buoyant plume, s
$\tilde{t}_{Mf}$	travel time to final rise of a pure momentum jet, s
t_r	release time interval over which mass W_r is emitted, s
U	windspeed at height z above ground, m/s
u'	root mean square x direction turbulence velocity, m/s
U_c	average convection windspeed through a plume y-z cross section, m/s
U_h	wind speed at the local plume height h, m/s
u_s	RMS turbulence velocity scale; usually u', v', or w', m/s
v'	root mean square y direction turbulence velocity, m/s
v_e	entrainment velocity
w'	root mean square z direction turbulence velocity, m/s
W	vertical mean velocity of the plume, m/s
W_s	mean velocity of the vertically directed jet at the "source", after pressure outside the pipe exit adjusts from P_e to P_a, m/s
x	downwind distance from source, m
x_r	$t_r U_c$, release length of a transient plume, m
y	crosswind distance from plume axis, m
z	height above ground level, m
z_r	reference height for turbulence scale evaluation in a boundary layer, see (3-9), m

z_{ref}	reference height for turbulence scale evaluation in inertial subrange model, see (3-9), m
z_o	roughness height parameter in log-law velocity profile, m

Greek

α	1) strength of the concentration fluctuation variance sink used to model surface layer $\overline{c'^2}$ dissipation, see (3-15) 2) also: entrainment constant for a jet with no crosswind bending-over, see Figure 4-1
β	entrainment constant for a bent-over plume or momentum jet, see Figure 4-1.
ε	dissipation rate of atmospheric turbulence m^2/s^3
$\overline{\varepsilon}$	dissipation rate of self-generated internal plume turbulence, m^2/s^3
ϕ_z	0.706 σ_z, vertical displacement of the effective concentration fluctuation variance source above the actual source height, for a ground level release
γ	intermittency factor; fraction of time that non-zero concentrations are observed at a fixed receptor
γ_h	intermittency factor on plume axis at y = o and z = h
ρ	density of ambient air, kg/m^3
ρ_s	density of gas at the "source" condition, at atmospheric pressure P_a after any expansion from pipe exit pressure P_e has occurred, kg/m^3
σ_{iy}	ensemble averaged instantaneous crosswind spread, m
σ_{iz}	ensemble averaged instantaneous vertical spread, m
σ_{my}	meandering component of total crosswind spread, see (2-1), m
σ_{mz}	meandering component of total vertical spread, see (2-1), m
σ_s	apparent source size "spread", m
σ_{self}	plume spread due to self-generated turbulence caused by jet momentum and buoyancy, see (4-11), m
σ_x	total, time or ensemble averaged along-wind spread, m
σ_y	total, time or ensemble averaged crosswind spread, m

λ	$(\sigma_y\sigma_z)^{0.5}/H$, normalized plume spread; used to characterize downwind distance
Λ_f	integral Eulerian length scale of along-wind turbulence velocity u in the x direction, m
λ_o	virtual origin displacement used to account for the effect of source size on concentration fluctuation intensity, see (3-1) and (3-2)
λ_s	virtual origin for source size effects on concentration fluctuation intensity in inertial surange model, see (3-4) and (3-5)
λ_{sp}	virtual origin for conditional fluctuation intensity, see (3-19) and (3-20)
Λ	$(\Lambda_v + \Lambda_w)/2$, average integral scale of turbulence contributing to plume spread, m
Λ_v	integral Eulerian length scale of crosswind turbulence velocity v in the x direction, m
Λ_w	integral Eulerian length scale of vertical turbulence velocity w in the x direction, m
σ	crosswind plume spread caused by the combined effects of self-generated and atmospheric turbulence, see (4-12), m
σ_{zc}	vertical plume spread caused by the combined effects of self-generated and atmospheric turbulence, see (4-12), m
σ_z	total, time or ensemble averaged, vertical spread, m
τ_e	decay time constant for a transient release, see (2-8), s

EXECUTIVE SUMMARY

This report is the fifth in a series which began in 1979 with "The Release and Dispersion of Gas from Pipeline Ruptures". These reports have concentrated on developing analytical methods for predicting the rate of release, plume rise, and atmospheric dispersion of toxic or flammable gas from a high pressure pipeline rupture or well blowout. The dispersion model which has been formulated predicts not only the mean concentration but also the probability of exceeding specified peak values. This report deals with four distinctly different aspects of this dispersion model. The new analytical methods developed and the conclusions drawn from them are summarized below.

Puff Versus Plume Models for Transient Releases

An accidental release is usually a short term transient event that lies somewhere between an instantaneous puff and a continuous plume. Puff and plume models are examined to show that during the early stages of dispersion the long sausage shaped release from a suddenly started and stopped source behaves like a plume. Later, as along-wind dispersion entrains atmospheric air into the head and tail of this plume, the release behaves like a large puff. During the transition period from plume to puff behavior both theoretical models overpredict the concentration in the transient plume and provide a conservative estimate for concentration. Because both puff and plume models are conservative, it is recommended that the predicted concentration be taken as the smallest of the values computed by puff and plume approximations to the transient release. This approach should simplify the risk analysis procedure.

The Effect of Source Size on Concentration Fluctuations in Plumes

The diameter of the source plays an important role in determining the peak values of fluctuating concentrations because plumes from small diameter sources

tend to meander back and fourth in large scale atmospheric turbulence and produce higher peak concentrations than those from large sources. The most important variable is the ratio of the source diameter to the scale of atmospheric turbulence. A new theoretical model for the effect of source size is developed by considering the interaction of the plume with atmospheric turbulence. Because this new approach makes direct use of atmospheric turbulence scales, it should have more general applications than the previous model of Wilson (1982) which is based on experimental data from wind tunnel simulations.

For high speed jets from pipeline ruptures, the emerging jet entrains ambient air and expands in size before it has been slowed down enough to be influenced by atmospheric turbulence. A simple theoretical model is developed to deal with this effect, and it is shown that the effective source size from a high pressure rupture may be a hundred times or more larger than the pipe exit diameter. This larger effective source size reduces the probability of being exposed to high peak concentrations in the plume far downwind.

Dilution by Self-Generated Turbulence Near the Source

The high velocity buoyant jet from a pipeline rupture will generate turbulence due to its momentum and buoyancy. Air entrainment from this self-generated turbulence causes the plume to be diluted even in the absence of atmospheric turbulence. Estimates are made for the rate at which this dilution occurs in the high speed jet near the source, and in the plume after it has been bent over by the wind. The theory predicts that as the plume enters its bent-over phase, ambient air entrainment by self-induced jet turbulence causes dilution of a hundred-fold or more in source concentration. However, atmospheric turbulence eventually becomes the dominant factor in dispersion, and by the time

the point of maximum ground level concentration is reached, the effect of self-generated turbulence on dilution is generally negligible.

Combining Momentum and Buoyancy Contributions to Plume Rise

Well defined methods are available to predict the combined effects of vertical jet momentum and buoyancy on the plume rise during its initial bent-over phase when it is influenced entirely by self generated turbulence. However, once the plume interacts with atmospheric turbulence and levels off at a final rise height, there are no methods for predicting this final rise which combine both the effects of momentum and buoyancy. For stack design, the usual approach has been to neglect the source momentum and compute only the final buoyancy rise. However, for the high velocity release from a pipeline rupture or well blow-out, jet momentum may contribute a significant fraction of the total final rise. To account for this, theoretical estimates for final rise developed by Briggs (1975) are extended to account for both momentum and buoyancy effects. The theory which results is complicated, and a simple approximation is suggested in which the separate momentum jet and buoyant plume final rises are added using a sum-of-cubes law. This simple approximation is shown to yield accurate final rise predictions within $\pm$ 10% of the exact theoretical value.

CHAPTER 1

INTRODUCTION

Plumes from high pressure pipeline ruptures or well blowouts are considerably different from the stack gas plumes to which most dispersion models are tuned. Some important differences between analyzing stack gas plumes and dispersion from pipeline ruptures are:

- The release rate from a pressure vessel or pipeline will decrease with time as the pressure in the system drops. This will produce a transient plume whose dispersion characteristics will lie somewhere between that of an instantaneous puff release, and a steady plume.

- The high internal pipeline pressure will cause the flow to choke at sonic velocity at the pipe exit, and to suddenly expand and accelerate outside the exit as it comes into equilibrium with atmospheric pressure. Both the release rate and outside expansion require the use of compressible gas dynamics to estimate mass and momentum fluxes.

- The high velocity jet from a rupture will undergo considerable dilution due to internally generated turbulence before it is bent over by the wind and dispersed by atmospheric turbulence.

- Most accidental ruptures occur at ground level, and the plume from a high velocity ground level source behaves differently than a buoyant plume from a high stack. Some method must be found to include both the effects of jet momentum and buoyancy on the trajectory and final rise of a high velocity pipe rupture release.

- Concentration fluctuations are present in all plumes dispersed by turbulence. However, it is of crucial importance to accurately estimate these fluctuations for the highly toxic gases that may be released from pipeline ruptures and well blowouts to determine the risk of exposure to high peak levels. Because these fluctuations depend strongly on the source size and conditions at the point of release, as well as the intensity and scale of the atmospheric turbulence which disperses the plume, accurate estimates are much more difficult to obtain than for mean concentrations.

To account for these differences a study was carried out which resulted in the report "The Release and Dispersion of Gas From Pipeline Ruptures" (January

1979). At that time there was little theory and almost no experimental data on which to base a release rate and dispersion model for pipeline ruptures. The report recognized this and took the point of view that "it is better to make an estimate, which may be at best an educated guess, than to ignore the effect of a parameter entirely." The fundamental assumptions on which the model was based have remained suprisingly durable in spite of the large measure of educated (and sometimes desperate) guesswork that went into its formulation. A series of subsequent reports; "Expansion and Plume Rise of Gas Jets from High Pressure Pipeline Ruptures" (April 1981), "Predicting Risk of Exposure to Peak Concentrations in Fluctuating Plumes" (December 1982) and "Exposure Time Effects on Concentration Fluctuations in Plumes" (January 1985) have modified and refined the theory and compared it with both full scale and wind tunnel data.

This report is the fifth in this series. Its purpose is to develop further the analytical methods in the existing theoretical model. While its general focus is on the dispersion of toxic gas from pipeline ruptures, many of the theoretical relations that are developed can be applied equally well to other atmospheric dispersion situations. An attempt has been made to review the existing results before presenting new theories or recommending changes. Hopefully, this will allow the report to make sense without the need for the reader to constantly refer to the previous reports in the series.

CHAPTER 2

DISPERSION FROM TRANSIENT RELEASES

The release of toxic or flammable gases is usually a short term event that occurs over a time interval of a few seconds to a few hours. The situation is further complicated by release rates which vary with time, for example the case of an exponentially decreasing release from the rupture of a high pressure vessel or pipeline. In this chapter we will develop methods for dealing with transient releases within the traditional framework of atmospheric dispersion of continuous steady plumes and instantaneously released puffs.

Limiting Cases: Puffs and Steady Plumes

A very short duration release can be modelled as an instantaneous puff, while at the other extreme, a release of long duration may be thought of as a steady plume, except near its "nose" and "tail" where it starts and stops. There are two fundamental differences between a puff and a plume, one related to its geometry and the other to the way in which its spread is measured. A puff spreads in all three dimensions, x, y and z as it is carried downwind, while a plume is diluted only by its crosswind spreading in y and z. The alongwind spreading of the series of puffs that make up a plume is ineffective in causing dilution because it is material from the puffs immediately upwind and downwind that is being entrained, rather than fresh air.

The ensemble averaged dispersion σ_{iy} of a puff is measured relative to the mass center of each of the puffs in the ensemble. Because the spread is relative to the mass centers of the puffs it does not include dispersion σ_{my} caused by meandering of the mass centers themselves. A receptor fixed on the

ground will see dispersion caused by both σ_{iy} and σ_{my} as it is exposed to the passage of an ensemble of puffs. The total crosswind spread σ_y will be

$$\sigma_y^2 = \sigma_{iy}^2 + \sigma_{my}^2 \qquad (2\text{-}1)$$

where

σ_{iy} = crosswind "instantaneous" spread of puffs to their mass centers

σ_{my} = crosswind "meandering" spread of the mass centers of the ensemble of puffs

Because a continuous plume is just a series of superposed puffs the same definitions apply, with the instantaneous spread found by taking an ensemble of snapshots, and measuring σ_{iy} relative to the centroid of each instantaneous concentration profile. The total dispersion is found either by taking a long time exposure, or by measuring the meandering of the centroids of each ensemble of snapshots and using (2-1).

The important distinction between the spread of puffs and plumes is simply one of terminology. The term "spread" used in the literature is almost always used to refer to the instantaneous "relative" dispersion of a puff and to the total dispersion of a continuous plume. Unless this difference is understood a great deal of confusion can result in interpreting puff and plume spreads reported in the literature. From the standpoint of risk analysis, we are interested in a fixed receptor on the ground, and the dispersion of an ensemble of puffs is the same as that of a plume, and includes both the instantaneous and meandering spreads.

The geometrical differences between puff and plume dispersion appear explicitly in the equations for maximum concentration at the center of an ensemble of puffs, each of which has a total mass release of m_r, kg.

$$C_{puff} = \frac{m_r}{(2\pi)^{3/2}\ \sigma_x\ \sigma_y\ \sigma_z} \qquad (2\text{-}2)$$

For the same mass released slowly over a long time duration t_r the dispersion may be modelled as a continuous plume, with

$$C_{plume} = \frac{Q}{2\pi\ U_c\ \sigma_y\ \sigma_z} \qquad (2\text{-}3)$$

where $Q = m_r/t_r$ is the source strength. Taking the ratio of (2-3) to (2-4) and defining a release length $x_r = t_r U_c$, where U_c is the mean convection velocity of plume material through a plume crosswind section, we obtain

$$\frac{C_{plume}}{C_{puff}} = (2\pi)^{1/2} \left(\frac{\sigma_x}{x_r}\right) \qquad (2\text{-}4)$$

The ratio is unity when $\sigma_x = (2\pi)^{-0.5}\ x_r$ which is $\sigma_x = 0.4\ x_r$. For short duration releases, where x_r is small, the plume model predicts higher concentrations than the puff model because the plume neglects the alongwind dispersion. For long duration releases the puff model yields higher concentrations because all the mass m_r is released instantaneously rather than spread out over a distance x_r.

Transition From Puff-like to Plume-like Dispersion

From the preceding discussion it is clear that at the two limits of short puff-like bursts and long plume-like releases, the correct model, (2-2) or (2-3) is the one which predicts the lowest concentration. That is, as a model becomes inappropriate it will tend to overestimate the concentration. This observation provides a simple way of choosing whether a release is

puff-like or plume-like; simply evaluate the concentration using both models and choose the one that yields the smallest concentration.

Another approach to defining a transition between puff and plume-like behavior is to examine how the upwind "nose" and downwind "tail" of a transient release modify the continuous plume between them. This situation is shown schematically in Figure 2-1 where the release is viewed from above after having travelled some distance downwind. The concentration distribution has a nose and tail that are influenced by σ_x and disperse like puffs. Between them is a region which behaves like a continuous plume, uninfluenced by the additional dilution of the nose and tail. As the release moves downwind, σ_x increases while x_r remains constant, and the nose and tail puffs gradually erode the plume-like core. For simplicity, we will assume that the plume-like core region disappears when $\sigma_x = (2\pi)^{-0.5} x_r$, which is the point where the plume and puff models in (2-4) predict the same concentration. From Figure 2-1 we see that the nose and tail merge when $R = 0.5\ x_r$, so that the effective "radius" of these puffs must be $R = (\pi/2)^{0.5}\ \sigma_x$, which seems reasonable.

The transition to complete puff-like behaviour requires the nose and tail zones to completely merge. Based on the experiments of Fackrell and Robins (1981) for ground level sources, the transition to puff-like behavior is complete when the nose (or tail) puff radius R has increased to about three times the critical value $(\pi/2)^{0.5}\sigma_x$ where the nose and tail puffs begin to merge. Using this observation, the criteria for release behavior are:

$$\begin{aligned} \sigma_x &\tilde{<} 0.4\ x_r, && \text{plume-like} \\ \sigma_x &\tilde{>} 1.2\ x_r, && \text{puff-like} \end{aligned} \qquad (2\text{-}5)$$

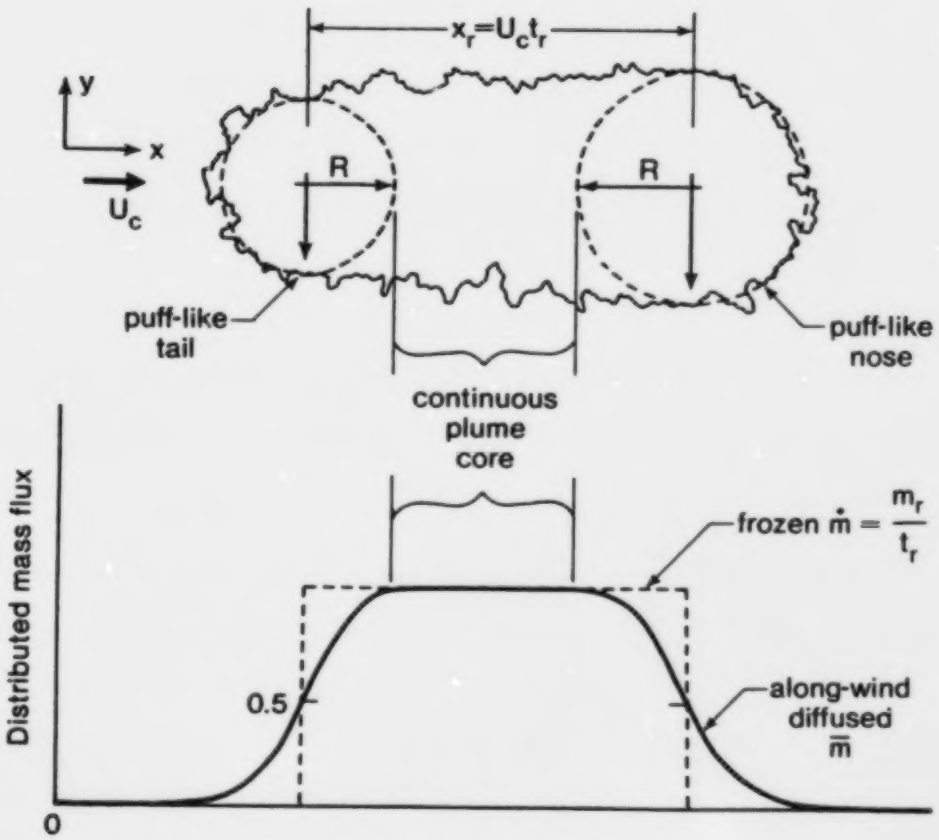

Fig. 2-1 Along-wind diffusion at the nose and tail of a transient suddenly started and stopped plume.

A release of fixed length $x_r = U_c t_r$ will behave initially as a plume, until along-wind diffusion of the nose and tail cause a transition to puff-like behaviour. Wilson (1981a.) gives a more rigorous treatment of diffusion in the nose and tail of a plume, and develops a plume model that includes an along-wind component.

The criteria in (2-5) are in good agreement with the wind tunnel data of Fackrell and Robins for diffusion of a large ensemble of 100 to 300 releases from a ground level source. These experiments also confirm that during the transition from plume-like to puff-like behaviour, both puff and plume models overestimate the concentration. The puff model overestimates concentration because it concentrates the release at a single instant, and the plume model also overestimates, because it neglects along-wind dispersion. Thus, selecting the smaller of the two predictions will always be conservative.

Characteristic Release Duration

The previous discussion considered the simplest type of transient release; a suddenly started and stopped steady release rate. Most practical situations, particularily accidental releases from pipe and pressure vessel ruptures, have a time-varying release rate $\dot{m}_e$. The choice of an appropriate release duration is not obvious, particularily for releases which start and stop for short periods during the release. Robins (1984) suggests that the best choice is the mass-weighted time centroid defined as

$$t_d = \frac{1}{m_r} \int_0^\infty \dot{m}_e \, t \, dt \qquad (2\text{-}6)$$

where m_r is the total mass released

$$m_r = \int_0^\infty \dot{m}_e \, dt \tag{2-7}$$

For an exponentially decaying release rate from a pipe rupture

$$\dot{m}_e = \dot{m}_{eo} \exp\left[-\frac{t}{\tau_e}\right] \tag{2-8}$$

it is easy to show that (2-8) yields

$$t_d = \tau_e \tag{2-9}$$

so that the characteristic release duration is equal to the decay time constant.

Estimating Along-Wind Spread

Predicting transition from plume-like to puff-like behaviour requires an estimate for the along-wind spread σ_x. This component of plume spread is strongly influenced by vertical wind shear dU/dz, which enhances the rate of spread. As the plume spreads vertically wind shear causes an along-wind separation of the plume layers, which are then smeared together by further vertical spreading. Wilson (1981a) shows that for a ground level source in a power law velocity profile with $U \propto z^n$ that the shear induced along-wind spread is

$$\sigma_{x_{shear}} = 0.6\, n\, (2.9)^n \times \sigma_z \tag{2-10}$$

so that the total along-wind spread is

$$\sigma_x^2 = \sigma_{x_{turbulence}}^2 + \sigma_{x_{shear}}^2 \tag{2-11}$$

The strong x dependence of the shear component usually makes it the dominant term.

It is interesting to note that for $\sigma_z \propto x^{1/2}$ the wind shear component in (2-10) predicts that $\sigma_x \propto x^{3/2}$. This is the same exponent predicted for relative dispersion of puffs in the inertial subrange of turbulence, and some of the data reported by Gifford (1977) which shows this accelerated spreading may in fact be dominated by wind shear rather than turbulence.

Estimating Instantaneous Plume or Puff Spread

In the previous discussion the total spread σ_y in (2-1) was shown to be the appropriate parameter to describe the dispersion of an ensemble of puffs or instantaneous plumes relative to a specific fixed receptor on the ground. However, only the instantaneous spread σ_{iy} represents real dilution of source material by entrainment of ambient air. The meandering component σ_{my} is generated by large scale atmospheric turbulence flapping the instantaneous plume (or a series of puffs) back and forth over the receptor. This random motion of the plume or puff mass center causes an apparent dispersion to a fixed observer, as the plume material meanders away to contaminate some other receptor location.

In a situation where there is no specific receptor location, for example in estimating the general toxicity or flammability hazard at a given radius from a source, it is more useful to use the instantaneous plume spreads σ_{iy} and σ_{iz} as measures of dilution. Because atmospheric diffusion models used in design and regulation of emissions predict only the total plume spreads, an estimate of instantaneous spread in terms of the total spread is the most useful form in which to express σ_{iy}. A detailed discussion of functional relationships for total and instantaneous spread is given in Appendix A where it is shown that total spread responds to the turbulence spectrum with high

frequency components filtered out, and instantaneous spread to a band-pass filter that removes both high and low frequency components. Both σ_y and σ_{iy} share a dependence on the crosswind turbulence intensity v'/U_c, the Eulerian turbulence scale Λ_v and its Lagrangian counterpart, L_v.

In terms of the turbulence intensity and scale, the power law equation for crosswind spread is given by (A2)

$$\sigma_y = \left[D_y^2 \, x^{2a_y} + \sigma_s^2 \right]^{0.5} \tag{2-12}$$

with the constant given by (A8)

$$D_y = (2A_1 \, \Lambda_v)^{1-a_y} \left[\frac{v'}{U_c} \right]^{a_y} \tag{2-13}$$

with a value of $A_1 \simeq 0.6$ recommended by Pasquill (1974), pp. 89-92.

In this equation the effect of source size σ_s is added in the form of a random uncorrelated variance to the turbulent spread. This random contribution of source size is a consequence of a fundamental assumption in the statistical theory of dispersion, which simply tags fluid particles as they pass the source location. These tagged "source" particles immediately take on the turbulence properties of the diffusing flow and account for source size only as a random variable on initial particle position. This leads to source size appearing as an additive variance in (2-12).

Most real sources are formed by a fluid jet, which remains coherent after release. Some distance after release is required before the turbulence velocities and scales of the diffusing flow become dominant and decorrelate the internal flow structure of the source jet. For real sources a linear addition of source size may be a better approximation, and (2-12) takes on the form

$$\sigma_y = D_y x^{a_y} + \sigma_s \tag{2-14}$$

If the instantaneous plume spread is dominated by turbulence in the inertial subrange, it is predicted by (A28) in Appendix A

$$\left[\frac{\sigma_{iy}}{\Lambda_v}\right]^2 = \left[\left[\frac{2}{3A_1}\right]^{1/3} \left(\frac{v'}{U_c}\right) \frac{x}{\Lambda_v} + \left[\frac{\sigma_s}{\Lambda_v}\right]^{2/3}\right]^3 \tag{2-15}$$

which for $\sigma_s = 0$ reduces to the expected relationship, $\sigma_{iy} \propto x^{3/2}$. This equation is valid only for spreading close to the source where the plume or puff width is small compared to the turbulence scale Λ_v. In these circumstances the total spread grows linearly with x, so that $a_y = 1.0$. Using this value in (2-13) and (2-14)

$$\sigma_y = \left(\frac{v'}{U_c}\right) x + \sigma_s \tag{2-16}$$

near the source. Using (2-16) in (2-15) the ratio of instananeous to total spread is given by

$$\frac{\sigma_{iy}^2}{\sigma_y^2} = \left[\left[\frac{3}{2A_1}\right]^{1/3} \left[\frac{\sigma_y}{\Lambda_v}\right]^{1/3} \left[1 - \frac{\sigma_s}{\sigma_y}\right] + \left[\frac{\sigma_s}{\sigma_y}\right]^{2/3}\right]^3 \tag{2-17}$$

which is valid for $\sigma_{iy} \ll \Lambda_v$. For the full turbulence spectrum, the result is more complicated. Using (2-16) in (A40)

$$\frac{\sigma_{iy}^2}{\Lambda_v^2} = \left[\left[16 + 8\left[\left[\frac{2}{3A_1}\right]^{1/3}\left[\frac{\sigma_y}{\Lambda_v} - \frac{\sigma_s}{\Lambda_v}\right] + \Phi_s\right]^{1/2} - 4\right]\right]^3 \tag{2-18}$$

which should be valid as long as $\sigma_{iy} < \Lambda_r$. The source size factor is, Φ_s from (A-39)

$$\Phi_s = \left[\frac{\sigma_s}{\Lambda_v}\right]^{2/3} + \frac{1}{8}\left[\frac{\sigma_s}{\Lambda_v}\right]^{4/3} \qquad (2\text{-}19)$$

Experimental Verification of Instantaneous Spread Predictions

Although there is a great deal of experimental data on total and instantaneous plume spreads, only the data of Nappo (1984) presents measurements of both quantities in the same flow, along with the turbulence statistics needed to test the predictions of (2-17) and (2-18). Nappo used photography to record an ensemble of 16 instantaneous snapshots of smoke plume dispersing in grid turbulence in a wind tunnel. These 16 independent realizations used to measure instantaneous spreads were taken at 15 second intervals during which a 4 minute time exposure was recorded to measure total spread. Nappo's objective was to deduce turbulence intensity and scale from the observed smoke plume spreads. Here we will use the measured spreads and turbulence statistics from hot wire anemometer measurements to test the equations for estimating instantaneous spread.

The turbulence grid used by Nappo was a square bar, square mesh biplane grid with a mesh size of 10 cm and a bar size of 2 cm. Square plates 30 x 30 cm were used to block 9 adjacent holes out of every 36 to create high intensity large-scale turbulence. A circular tube with an inside diameter of 0.873 cm injected smoke isokinetically into the flow 400 cm downstream from the grid. Measurements of vertical spreads σ_{iy} and σ_y were made by Nappo from photographs at 8 locations from x = 25 cm to x = 350 cm.

There are were two major obstacles in comparing Nappo's measurements with the theory. The first is the natural decay of grid turbulence with downstream distance. The x direction intensity and scale varied from $u'/U \approx 0.13$ and $\Lambda_f \approx 21$ cm at the source to 0.07 and 33 cm at $x = 400$ cm. In contrast, the theoretical predictions assume homogeneous turbulence with constant intensity and scale. The second obstacle is that only x direction turbulence statistics were measured, using a single sensor hot film anemometer. This required the cross-stream statistics to be estimated from along wind values. Grid turbulence is generally anisotropic in intensity but has integral scale relations that are close to isotropic. For grid turbulence we estimated that $u'^2 \approx 2w'^2 \approx 2v'^2$, and that along-wind and crosswind scales were isotropically related, with $\Lambda_v \approx 0.5\ \Lambda_f$. With the scales estimated by fitting exponentials to Nappo's autocorrelations, the average intensity and scale over the 350 cm plume length was found to be $v'/U \approx 0.067$ and $\Lambda_v \approx 16$ cm.

Nappo's measurements for total plume spread were used to obtain a refined estimate of turbulence intensity and effective source size. The data are shown in Figure 2-2 where they are in good agreement with (2-16) with $v'/U_c = 0.062$ $\sigma_s = 0.70$ cm, and $A_1 = 1.0$ for grid turbulence as measured by Snyder and Lumley (1971). Because intensity and scale are inversely related in grid turbulence, this lower effective intensity implies a larger effective scale see (A6), and $\Lambda_v = 17$ cm was taken as the refined estimate.

Figure 2-2 shows the predictions of (2-17) and (2-18) using these values for intensity, scale and source size. The strong effect of source size on the instantaneous spread is evident, as well the persistent difference between instantaneous and total spreads. In general the experimental results are in good agreement with the full spectrum predictions.

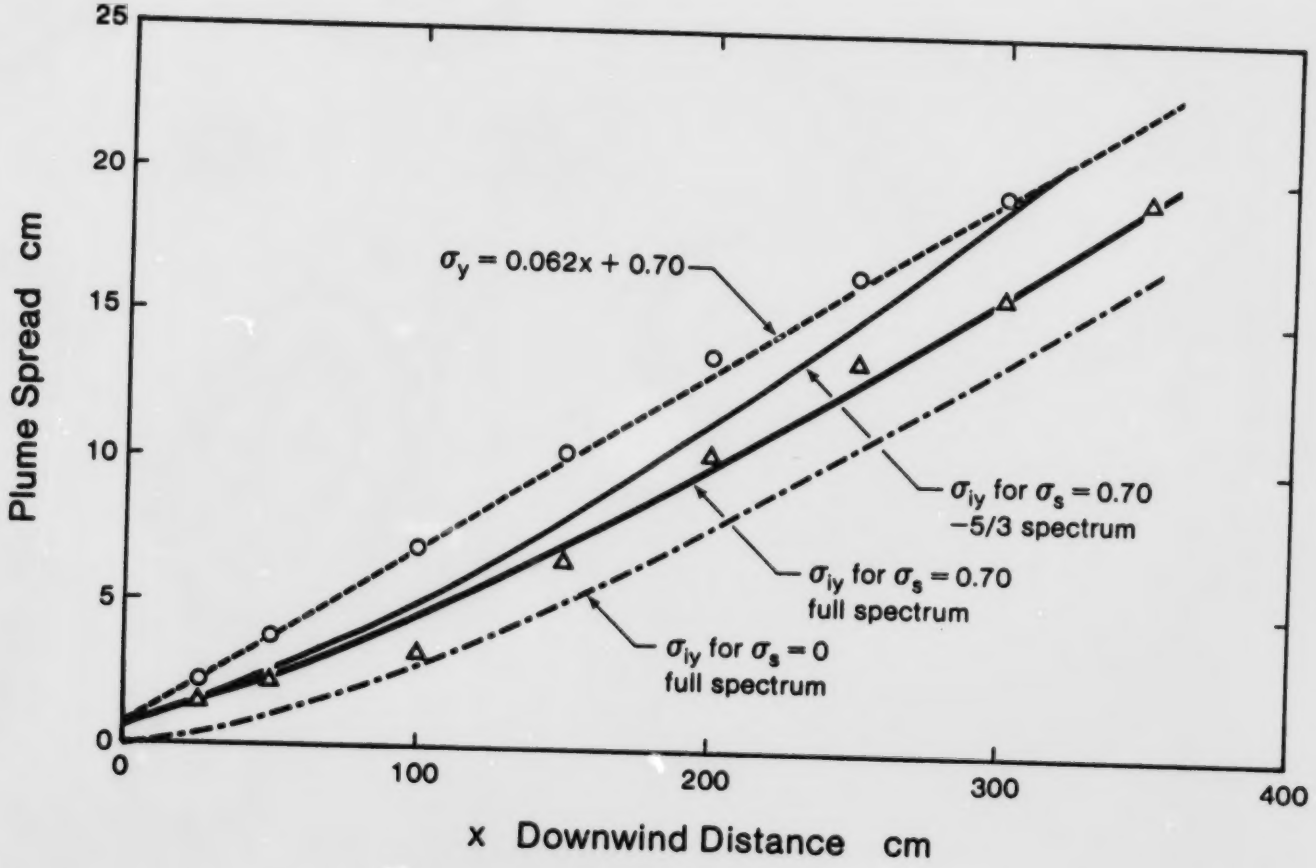

Figure 2-2 Instantaneous σ_{iy} (triangles) and time-averaged σ_y (circles) spread of a plume from a d = 0.7 cm source in grid turbulence. Data from Nappo (1984). Theory from (2-15), (2-16) and (2-18), (2-19) with $A_1 = 1.0$, $v'/U_c = 0.062$ $\Lambda_v = 17$ cm

Other theoretical estimates are available for the instantaneous to total plume spread ratio. Hanna (1984) used Gifford's (1982) Langevin equation formulation to solve for ratio of instantaneous to total spread,

$$\frac{\sigma_{iy}^2}{\sigma_y^2} = 1 - \frac{0.5\, S_1 (1 - \exp(-T'))}{\frac{1}{2A_1^2}\left[\frac{\sigma_s}{\Lambda_v}\right]^2 + T' - (1 - \exp(-T'))} \qquad (2\text{-}20)$$

where

$$T' = \frac{1}{A_1}\left(\frac{v'}{U_c}\right)\frac{x}{\Lambda_v}$$

and $A_1 \approx 0.6$ is the Eulerian-Lagrangian scale ratio constant in (A6). For most practical situations where $\sigma_s/L_v < 0.1$, Hanna shows that $S_1 \approx 1.0$ is a good approximation.

Figure (2-3) shows a comparison of Hanna's equation and our theory from (2-17) and (2-18) with Nappo's experiments. As expected, the approximation of the spectrum as an inertial subrange (- 5/3 spectrum) applies only very close to the source where $\sigma_{iy} \ll \Lambda_v$. Hanna's theory predicts much smaller values of the instantaneous to total spread ratio near the source. In part this is due to the use of an effective source size derived from a linear source correction in (2-14). If an additive variance is assumed, using (2-12), we find the total spread is well represented by $v'/U_c = 0.067$ and $\sigma_s = 1.4$ cm. With these values and $\Lambda_v = 16$ cm Hanna's model in (2-20) performs better, predicting a minimum variance ratio of 0.20 at x = 60 cm, close to the observed value.

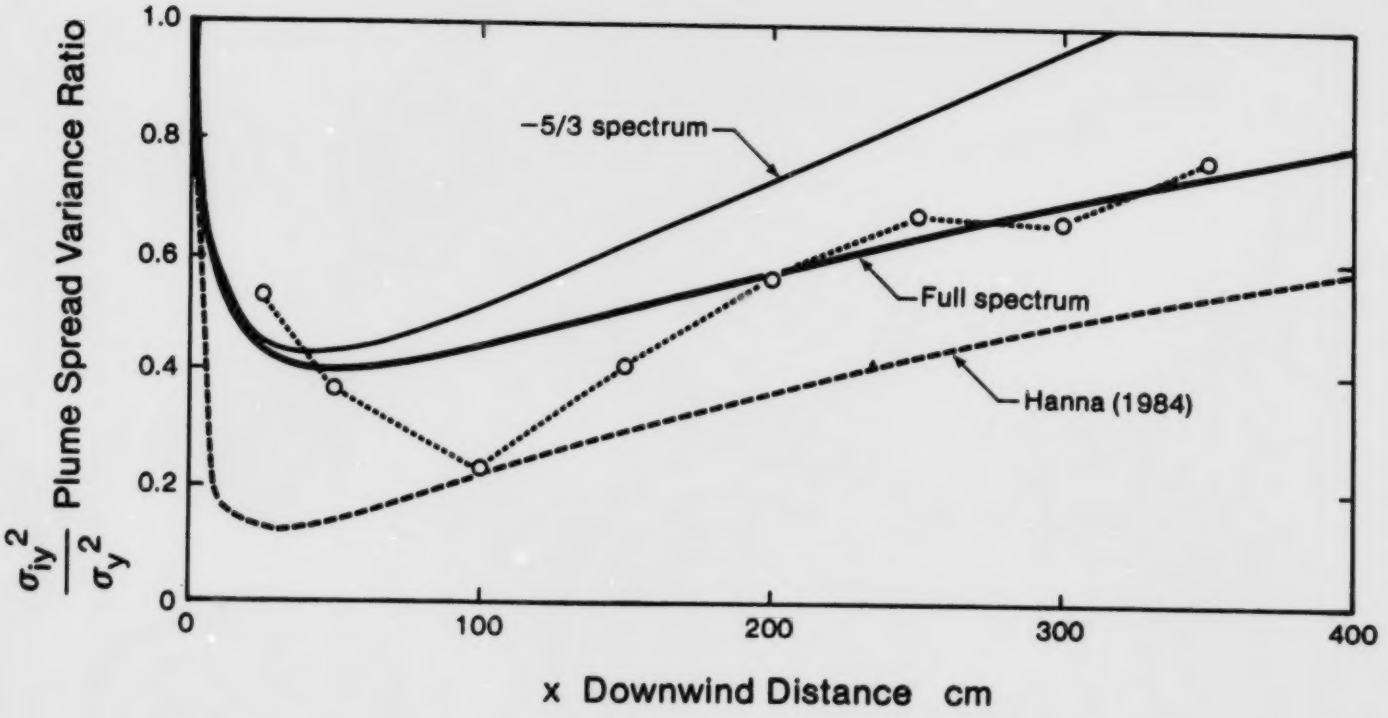

Figure 2-3 Ratio of instantaneous to total, time averaged, plume spread variances in grid turbulence experiments of Nappo (1984). Theory from (2-15), (2-16) and (2-18), (2-19). Hanna's theory from (2-20); σ_s = 0.7 cm, A_1 = 1.0, v'/U_C = 0.062, Λ_v = 17 cm

We conclude that either model gives an adequate representation of the ratio of instantaneous to total spread. Because Hanna's model always reduces to the correct asymptotic value of unity near to and far from the source, it is the preferred formulation. On the other hand, the model in (2-17) gives a better physical insight into the influence of the turbulence spectral bandpass on instantaneous spread.

Summary

In this chapter a set of criteria have been developed to mark the transition of a release from its initial plume-like behaviour to puff-like dispersion farther downwind. Because a plume dispersion model using σ_{iy} will always overestimate the concentration through its neglect of along-wind diffusion, the use of plume models for transient releases will give conservative estimates of exposure hazards.

Dispersion relative to the instantaneous center of mass of a puff or plume concentration profile is shown to be a useful way of characterizing the actual dilution of source material. Relationships between this instantaneous spread, and the total spread which contains the meandering component of dispersion are developed. By relating instantaneous to total plume spread the readily available total spread relations in each atmospheric stability class can be directly applied to hazard assessment.

CHAPTER 3

SOURCE SIZE EFFECTS ON CONCENTRATION FLUCTUATIONS

The most remarkable characteristic of concentration fluctuation intensity is its sensitivity to the geometry and release conditions at the source. To an engineer whose experience dictates that the influence of source geometry on a jet is limited to distances less than 50 source diameters, it seems incredible that concentration fluctuations will be influenced by source size at distances several kilometers downwind. However, for small elevated sources dispersing in the large scale atmospheric turbulence above the surface layer, this strong sensitivity is certainly present, and increases the difficulty in predicting peak concentration levels.

The physical mechanism behind this source size sensitivity lies in the difference between instantaneous plume spread and meandering. The source size acts as a filter which determines the amount of small scale atmospheric turbulence that will be effective in diluting the plume by entrainment. The larger scales do not contribute to air entrainment but instead cause the narrow instantaneous plume to meander back and forth. This generates a high level of intermittency and produces a high concentration fluctuation intensity at a fixed receptor.

The instantaneous plume spread from a small source increases very slowly in large scale turbulence, because it filters out most of the turbulent velocity fluctuations. Because the width of an instantaneous plume from a small source remains small, it is subject to meandering for much longer distances than the plume from a large source. The details of this turbulence filtering are discussed in Appendix A.

When periods of zero concentration are neglected, and conditional mean and fluctuation statistics are measured, the effect of source size can generally be neglected, as shown by Wilson (1982) and Wilson, Robins and Fackrell (1985). The reason for this change from strong source size sensitivity for total variance to almost complete insensitivity for conditional variance is that meandering affects the plume by producing intermittent periods of zero concentration. When these are removed in computing the conditional statistics, the remaining small scale mixing process is much less dependent on source size.

Along-Wind Variation of Fluctuation Intensity

Even in homogeneous turbulence far from the influence of ground surface effects, concentration fluctuation intensity will vary with downwind distance. This variation is due to the balance between advection, production, diffusion and dissipation of the total variance $\overline{c'^2}$ as well as the decrease in the mean concentration $\overline{c}$. By using the experimentally observed balance between advection and dissipation of variance, and a simple model for the dissipation time scale, Wilson, Fackrell and Robins (1982) derived a relation for the total fluctuation intensity on the plume axis,

$$\hat{i} = \frac{0.34\lambda}{\lambda^2 + \lambda_o^2} \qquad (3\text{-}1)$$

where $\hat{i}$ is the total fluctuation intensity on the plume axis in the absence of wind shear or ground surface effects. By expressing the along-wind distance $\lambda = \sqrt{\sigma_y \sigma_z}/H$ in plume coordinates, the theory attempts to provide a universal formulation that may be valid for a range of atmospheric stability and surface roughness conditions.

The virtual origin λ_o accounts for the effect of source size on the total variance, and is determined by the ratio of source size, d, to the average integral scale of turbulence $\Lambda = (\Lambda_v + \Lambda_w)/2$. Wilson, Fackrell and Robins (1982) included this scale by using the ratio of source height h to diameter d in their equation for the virtual origin λ_o. For the experimental data set of Fackrell and Robins (1982a) used to determine constants in the theory, Robins (1979) reported values of these turbulence scales. This data may be approximately fit by $\Lambda = 0.6z$, for $z < 0.25$ H, where H is the thickness of the atmospheric shear layer. Using this, the empirical equation for the virtual origin is

$$\lambda_o = \frac{0.12}{1 + 0.055 \frac{\Lambda}{d}} \qquad (3\text{-}2)$$

To account for inhomogeneous shear flows, the scale Λ is evaluated at a reference height. In (3-1) and (3-2) the constants proposed by Wilson, Fackrell and Robins (1982) are adjusted by the factor 1.177 to account for the use of plume standard deviations $\sqrt{(\sigma_y \sigma_z)}$ rather than half widths $\sqrt{(\delta_y \delta_z)}$ as the distance parameter. Also, their original formulation expressed the along-wind variation in terms of a variance source strength ratio q/Q and a separation factor β (or ϕ) for the pair of variance sources. Both these factors are combined in the constant 0.34 in (3-1).

Sykes, Lewellen and Parker (1984) propose a model for the dissipation time scale that accounts <u>directly</u> for the effect of source size on total variance. In the appendix to their paper they derive a simple model for $\hat{i}$ that predicts the distance λ_{max} to maximum intensity as $\lambda_{max} \propto d^{2/3} \Lambda^{1/3} H^{-1}$. This result is a consequence of limiting the turbulence to the inertial sub-range of the turbulence spectrum where the kinetic energy of turbulence decays as the -5/3 power of frequency.

Sawford (1983a) (1983b) using random-walk Lagrangian particle statistics shows that it is the Lagrangian rather than the Eulerian turbulence scale that is important. Using the Eulerian to Lagrangian scale relation in equation (A6) from Appendix A, his results predict the distance x_{max} to maximum variance should be proportional to $d^{2/3}\Lambda^{1/3}(u_s/U_c)^{-1}$ where u_s is the RMS turbulent velocity scale. It is shown in Appendix B that the turbulence velocity scale u_s/U_c in x_{max} disappears when the plume spread coordinate λ_{max} is used.

In contrast, the empirical equation (3-1) of Wilson, Fackrell and Robins (1982) has a maximum intensity at $\lambda_{max} = \lambda_o$. For small source sizes where Λ/d is large, (3-2) yields $\lambda_o \approx 2.2\ d\ \Lambda^{-1}$, so that $\lambda_{max} \propto d\ \Lambda^{-1}$. This empirical fit to the wind tunnel data is limited to the range $4 < \Lambda/d < 40$. The difference between the theoretical prediction of $\lambda_{max} \propto d^{2/3}$ and the empirical equation with $\lambda_{max} \propto d$ is significant.

The greatest weakness of the virtual origin correction in (3-2) is that it is only an empirical correlation, tuned to one specific neutrally stable wind tunnel shear flow, with a surface roughness of $z_o/H = 4 \times 10^{-4}$, (about $z_o = 25$ cm in the atmosphere). In the next section we will attempt to reduce this deficiency by deriving relations for source size directly from turbulence parameters.

Source Size Effects Derived from Turbulence

The major contribution of Sykes, Lewellen and Parker (1984) to developing an improved theory for the along-wind development of concentration fluctuations was their suggestion that the dissipation time scale for $\overline{c'^2}$ should be governed by variables that influence the instantaneous plume spread, rather than the total plume spread which includes meandering. Because meandering moves the entire plume back and forth, it will not contribute to

dissipation, which is governed by processes that cause actual dilution of plume material.

They developed a scaling hypothesis for the portion u_{si} of the total RMS turbulence velocity u_s that is effective in contributing to the spread σ_i of the instantaneous plume, and suggested

$$u_{si} = u_s \left(\frac{\sigma_i}{\Lambda}\right)^{1/3} \tag{3-3}$$

This velocity scaling implies an inertial subrange turbulence spectrum with kinetic energy proportional to the -5/3 power of fluctuation frequency.

In Appendix B these scaling principles are used to develop a simple theory for along-wind variation of total fluctuation intensity. In homogeneous turbulence, with constant integral scale and RMS velocity the theory predicts in (B22)

$$\hat{i} = \frac{B_6 \left(\frac{\Lambda}{H}\right)^{a-1} \lambda}{(\lambda + \lambda_s)^a} \tag{3-4}$$

The effect of source size is contained in the virtual origin λ_s. For turbulence in the inertial subrange, the effect of source size and turbulence scale on λ_s is given by (B23). Because the source size σ_s must be proportional to source diameter, (B23) can be written as

$$\lambda_s = B_0 \left(\frac{d}{H}\right)^{2/3} \left(\frac{\Lambda}{H}\right)^{1/3} \tag{3-5}$$

For homogeneous turbulence, where Λ is a constant, the maximum intensity in (3-4) occurs at

$$\lambda_{max} = \frac{\lambda_s}{(a-1)} \tag{3-6}$$

at which point the maximum intensity on the plume axis is

$$\hat{i}_{max} = B_6\left(\frac{a-1}{a}\right)^{a}\left(\frac{\Lambda}{H}\right)^{a-1}\lambda_s^{1-a} \qquad (3\text{-}7)$$

The distance λ_{max} to maximum concentration from (3-5) and (3-7) is proportional to $d^{2/3}\Lambda^{1/3}H^{-1}$ which is in good agreement with the wind tunnel data reported by Fackrell and Robins (1982b) for an elevated source in a weak shear flow. The data of Fackrell and Robins (1982a) has a dependence on source size that indicates $\hat{i}_{max} \propto d^{-1/3}$, which implies from (3-5) and (3-8) that a = -1.5.

Accounting for Wind Shear and Inhomogeneous Turbulence

The Wilson, Fackrell and Robins model in (3-1) and (3-2) and the new theory of (3-4) and (3-5) were developed for homogeneous turbulence and no wind shear. Sawford's (1983b) Lagrangian particle tracking simulations identified two different effects of boundary layer turbulence on concentration fluctuations.

- As the plume moves downwind it will sample varying scales of turbulence. These varying scales will change the meandering process of the instantaneous plume, and alter the effect of scale on λ_s.

- The mean wind shear dU/dz stretches and distorts eddies, increasing their mixing rates and causing the fluctuation intensity to rapidly lose its dependence on source size.

Wilson (1982) suggests a simple correction to the theory to simultaneously account for effects of changing scales and of wind shear on the plume from an elevated source, emitted at z = h in a boundary layer. These effects are accounted for by evaluating the scale Λ used in (3-2) at a reference height z_r

$$z_r = h \exp\left[-\left(\frac{\sigma_z}{h}\right)^2\right] \tag{3-8}$$

with $\Lambda = 0.6\, z_r$ in (3-2) for the neutrally stable wind tunnel boundary layer data in the study. For a ground level source $\Lambda = 0$ from (3-8), and (3-2) becomes independent of source size.

Because this simple correction attempts to account for wind shear and varying turbulence scale with a single parameter, it is limited to shear flows where the turbulence scales and wind shear are linked together. This restriction may limit the model's application to near-neutral atmospheric stability. Sawford's (1983b) calculations suggest that an additional length scale proportional to $(H\, U^{-1}\, dU/dz)$ may be required to describe more complex flows.

For the inertial subrange model in (3-4) and (3-5) a single scale adjustment will also be used to account for both turbulence inhomogeniety and wind shear decorrelation. The wind tunnel data of Fackrell and Robins (1982a), used to set the model's constants, has a scale variation with height of $\Lambda \approx 0.6z$. For a ground level source, an appropriate choice of height at which to evaluate the effective scale is $z_{ref} = B_8\sqrt{\sigma_y \sigma_z}$, while for an elevated source far from the influence of surface reflection and dissipation effects $z = h$ is a logical choice. A simple interpolation equation between these limits is

$$z_{ref} = \left[h^2 + B_8^2\, \lambda^2 H^2\right]^{0.5} \tag{3-9}$$

Using the wind tunnel data, one set of contants that is physically realistic is: $a = -1.5$, $B_o = 0.8$, $B_6 = 2.5$ and $B_8 = 0.5$. Using these, (3-4) and (3-5) become

$$\hat{i} = \frac{2.5\,\lambda\,\left(\frac{\lambda_{ref}}{H}\right)^{0.5}}{(\lambda + \lambda_s)^{1.5}} \tag{3-10}$$

and

$$\lambda_s = 0.8\left(\frac{d}{H}\right)^{2/3}\left(\frac{\Lambda_{ref}}{H}\right)^{1/3} \tag{3-11}$$

with the reference scale evaluated from (3-9)

$$z_{ref} = h\left[1 + 0.25\left(\frac{\lambda H}{h}\right)^2\right]^{0.5} \tag{3-12}$$

Predictions using these equations are compared to the wind tunnel data in Figure 3-1. Agreement is not as good as the empirical fit shown in Figure 3-2 using equations (3-1) and (3-2) with the effective scale from (3-8). However, the assumptions used to derive (3-10), (3-11) and (3-12) have a stronger physical basis than the purely empirical fit, and should be more reliable when extrapolated to other atmospheric stabilities, surface roughness and source conditions. (Note that the predictions in Figures 3-1, 3-2, include ground surface interaction effects discussed in the following section.)

Both the empirical correlation model (3-1) and (3-2) and the inertial subrange formulation of (3-10) and (3-11) predict a constant asymptotic value for the intensity from a ground level source, in agreement with the measurements of Fackrell and Robins (1982a). However, this agreement is forced by the way in which the turbulence scale relations (3-8) and (3-12) were chosen and should not be regarded as a verification of the theory.

In homogeneous turbulence where Λ and Λ_{ref} are constant both models predict a decay rate $\hat{i} \propto \lambda^{-1}$ far downwind. This result is in striking contrast to the Lagrangian particle tracking simulations of Sawford (1983a) who predicts a constant asymptotic value of $\hat{i}$ in this situation.

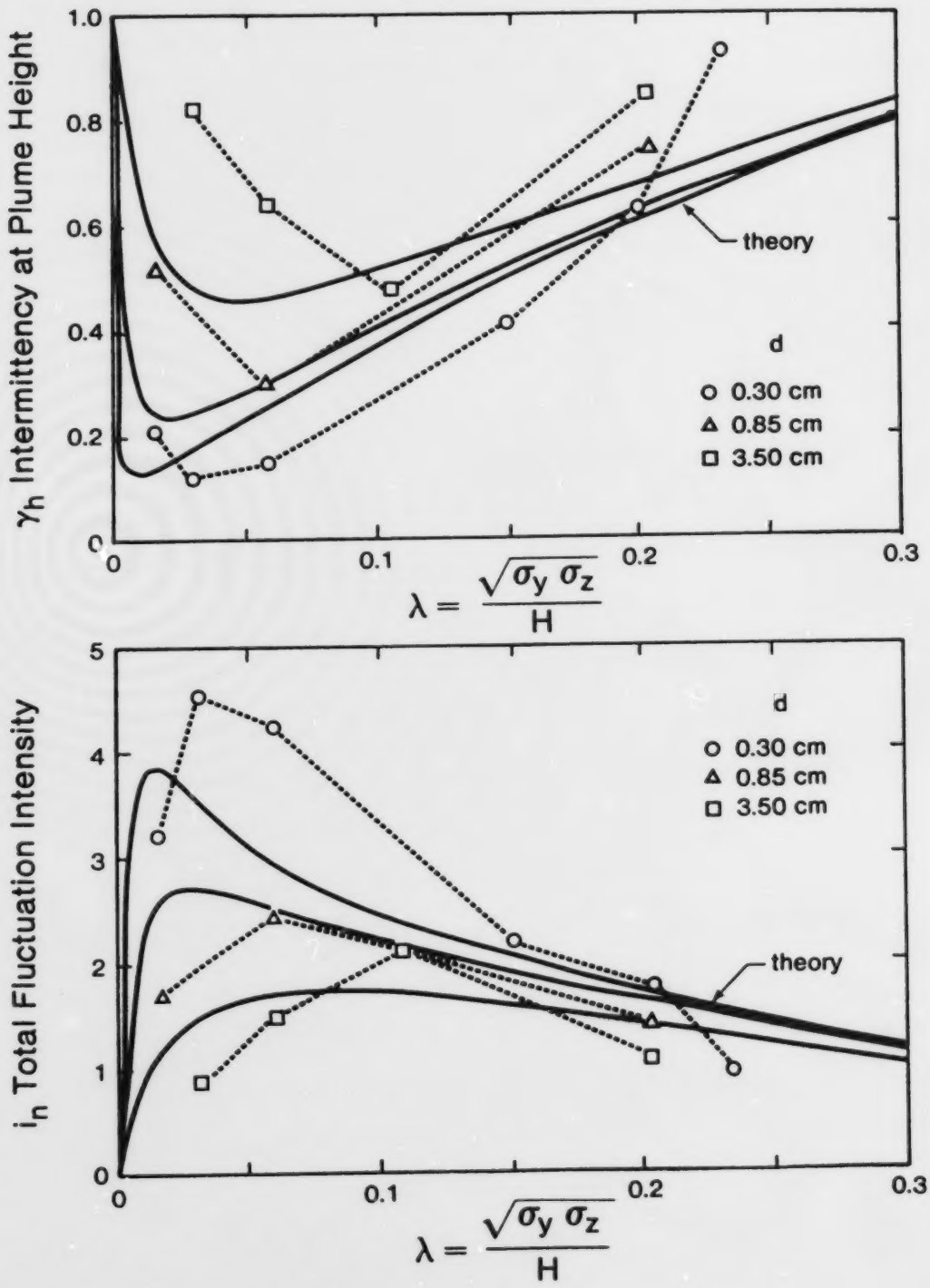

Fig. 3-1 Inertial subrange theory for intermittency and total concentration fluctuation intensity for an elevated source at h/H = 0.192 in a wind tunnel boundary layer of H = 120 cm. Data of Fackrell and Robins (1982a) theory from (3-10), (3-11), (3-12) and (3-13), (3-14), (3-15) with α = 0.6, ϕ_z = 0.706

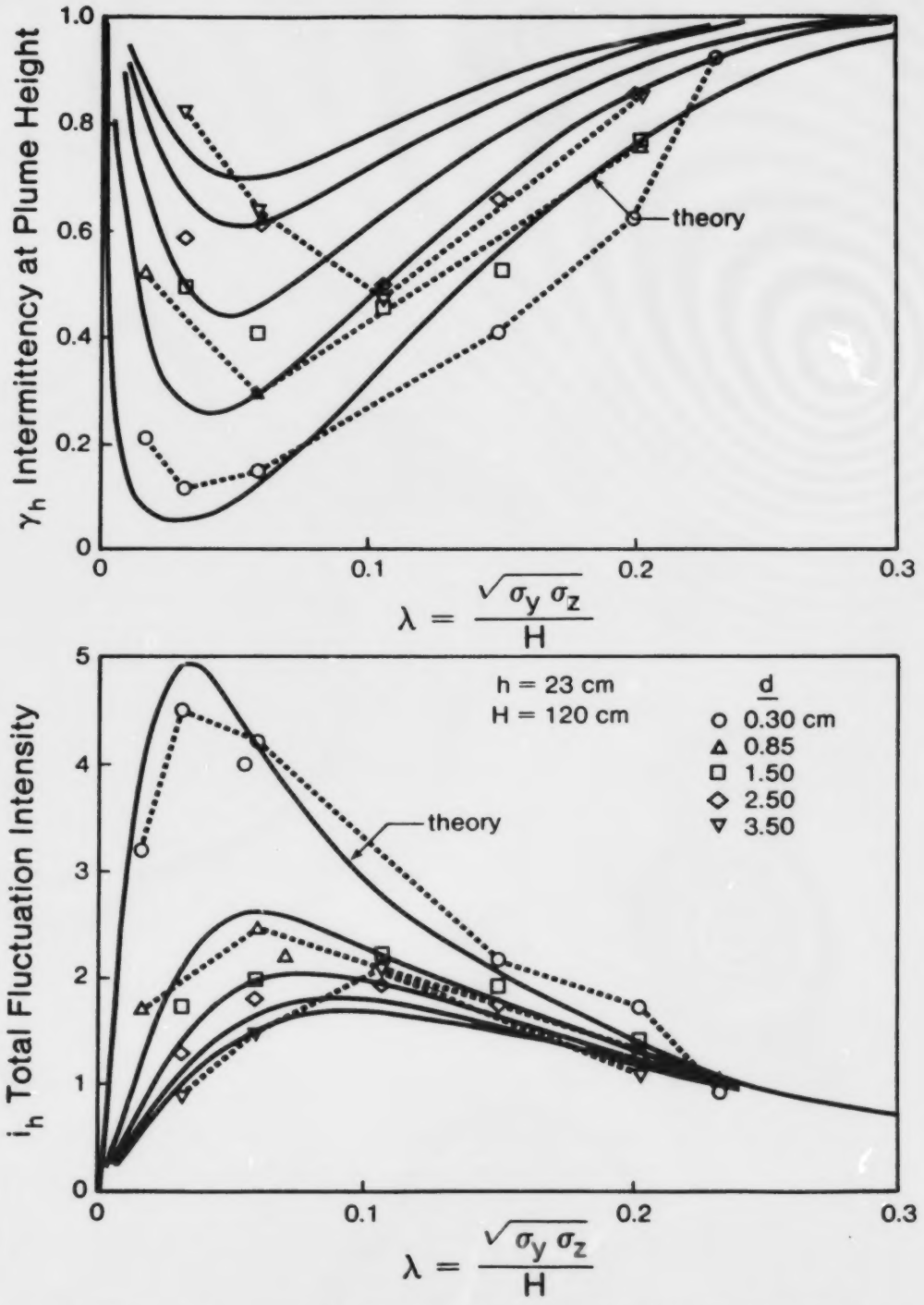

Fig. 3-2 Semi-empirical theory for intermittency and total concentration fluctuation intensity for an elevated source at h/H = 0.192 in a wind tunnel boundary layer of H = 120 cm. Data of Fackrell and Robins (1982a), theory from (3-1), (3-2) and (3-13), (3-14) and (3-15) with $\alpha = 0.6$, $\phi_z = 0.706$.

Unfortunately there are no experiments in homogeneous turbulence with which to resolve this difference. Grid turbulence, which is often used as an "approximately" homogeneous flow actually has a length scale Λ which increases with x, and behaves more like $\Lambda \propto \lambda$ than Λ = constant.

Surface Effects on Variance Profiles

Wilson (1982) approximates the spatial variation of both the mean $\overline{c}$ and variance $\overline{c'^2}$ profiles by Gaussian profiles. The effect of wind shear is modelled by using a single variance source displaced above the actual source height by an amount $\phi_z \sigma_z$, where ϕ_z = 0.706 was determined experimentally. The original theory in Wilson, Fackrell and Robins (1982) and Wilson (1982) used a pair of variance sources, which were located on either side of the point of release. However, Wilson and Simms (1985) later showed a single source gave more realistic predictions in the tails of profiles.

Near ground level, the presence of small scale turbulence and wind shear increase the rate of dissipation of concentration fluctuations. This surface layer dissipation is simulated in the model by an image sink for variance which has a strength equal to a fraction α of the variance source strength.

It is useful to consider the vertical source displacement and the image sink terms separately. For a source which is far above the surface, where neither the mean concentration image reflection source nor the variance image dissipation sink have any effect, it is easy to show from Wilson (1982) that

$$i_\infty = \hat{i} \exp\left[+\frac{y^2}{2\sigma_y^2}\right] \exp\left[\frac{-(z-h)^2}{2\sigma_z^2} - \frac{(z-h_v)^2}{4\sigma_z^2}\right] \qquad (3\text{-}13)$$

where $\hat{i}$ is the intensity in homogeneous turbulence, and i_∞ is the intensity in the absence of image sources and sinks. Note that i_∞ includes the

apparent vertical displacement h_v of the variance source

$$h_v = [\, h^2 + \phi_z^2 \sigma_z^2 \,]^{0.5} \tag{3-14}$$

with $\phi_z = 0.706$. Wilson (1982) gives the relationship between the intensity i at any location with the value i_∞ with no surface dissipation as

$$\frac{i}{i_\infty} = \frac{\left[1 - \alpha \exp\left[-\frac{2h_v z}{\sigma_z^2}\right]\right]^{0.5}}{1 + \exp\left[-\frac{2hz}{\sigma_z^2}\right]} \tag{3-15}$$

At the ground surface, z = 0 and this reduces to

$$\left.\frac{i}{i_\infty}\right|_{z=0} = \frac{(1 - \alpha)^{0.5}}{2} \tag{3-16}$$

$$= 0.316, \quad \text{for } \alpha = 0.6$$

independent of source height. On the centerline of a ground level source h = z = y = 0 and (3-13) reduces to

$$\left. i_\infty \right|_{h=0} = \hat{i} \exp\left[-\frac{\phi_z^2}{4}\right] \tag{3-17}$$

$$= 0.883\, \hat{i}, \quad \text{for } \phi_z = 0.706$$

Combining the surface dissipation and wind shear source displacement effects in (3-16) and (3-17) the ground level intensity from a ground level source is 0.28 $\hat{i}$, where $\hat{i}$ is the plume axis intensity in homogeneous turbulence, from (3-1) or (3-10).

Finally, it is interesting to compare this simple model with the results of Sykes, Lewellen and Parker (1984) who solved the complete differential equation for the variance field, using closure models for the various length

and velocity scales. They found that the boundary condition of $\partial \overline{c'^2}/\partial z = 0$ rapidly developed into profiles with steep gradients close to the surface. Their profiles were almost identical to the present model for both elevated and ground level sources. (Compare Figures 7 and 8 of Sykes, Lewellen and Parker (1984) to Figures 2 and 4 of Wilson, Fackrell and Robins (1982)).

Intensity of Conditionally Averaged Fluctuations

Wilson (1982) and Wilson, Robins and Fackrell (1985) develop a model for the conditionally averaged "plume" intensity, in which the intermittent periods of zero concentration are removed. The argument on which this model is based is that the total fluctuation intensity can be used to simulate the conditional intensity by a judicious choice of the effective turbulence scale Λ or Λ_{ref} in (3-1) or (3-10). The experimental data shows that for a ground level source $\gamma = 1.0$, on the plume centerline from which $\hat{i}_p = \hat{i}$ there.

For the model in (3-1) and (3-2), Wilson, Robins and Fackrell (1985) show that the appropriate choice of turbulence scale to simulate conditional averaging is $\Lambda = 0$, from which we obtain $\lambda_{op} = 0.12$ and the plume intensity

$$\hat{i}_p = \frac{0.34\,\lambda}{\lambda^2 + (0.12)^2} \qquad (3\text{-}18)$$

For the inertial subrange model in (3-10), and (3-11), a ground level source with $h = 0$ has $z_{ref} = 0.5\,\lambda H$. Using the scale relationship $\Lambda_{ref} = 0.6\,z_{ref}$ derived from the wind tunnel data, we find that $\Lambda_{ref}/H = 0.3\,\lambda$ for this case Using this scale in (3-10) and (3-11), the inertial subrange model predicts the conditional average intensity

$$\hat{i}_p = 1.37\left[\frac{\lambda}{\lambda + \lambda_{sp}}\right]^{1.5} \qquad (3\text{-}19)$$

where the virtual origin for the conditional intensity is at

$$\lambda_{sp} = 0.54\, \lambda^{1/3} \left(\frac{d}{H}\right)^{2/3} \qquad (3\text{-}20)$$

There are significant differences between the conditional "plume" intensities predicted by the empirical model in (3-18) and by the inertial subrange model in (3-19). The most important difference is that (3-19) and (3-20) predict a weak dependence of conditional intensity on source size for moderate travel distances. The model in (3-18) was purposely adjusted to have no source size dependence for conditional intensity $\hat{i}_p$.

Comparison with the experimental data in Figure (3-3) supports the weak dependence of $\hat{i}_p$ on source size. The inertial subrange model also shows a much more rapid increase in conditional intensity from its initial value of zero at the source. This is a considerable improvement over the Wilson, Robins and Fackrell (1985) prediction using (3-18) and shown in Figure (3-4) for comparison.

Effective Source Size for a Vertical Jet

What value should we use for the source size of a high velocity jet that is bent over by the wind? Clearly, atmospheric turbulence will not produce significant meandering or entrainment until the jet is slowed by its own self-generated turbulent entrainment to a speed where it can be bent over by the wind. As a rough estimate, we will assume that the jet acts like a passive isokinetic release once its vertical velocity W is equal to the mean windspeed U_h. At this point the jet will be bent over at an angle of 45°.

The momentum jet analysis in Appendix C shows that this occurs when the plume radius R is given by (C36). The effective source diameter d_{eff} for a vertical jet of velocity W and density ρ_s injected into a crosswind of velocity U and density ρ_a is from (C36)

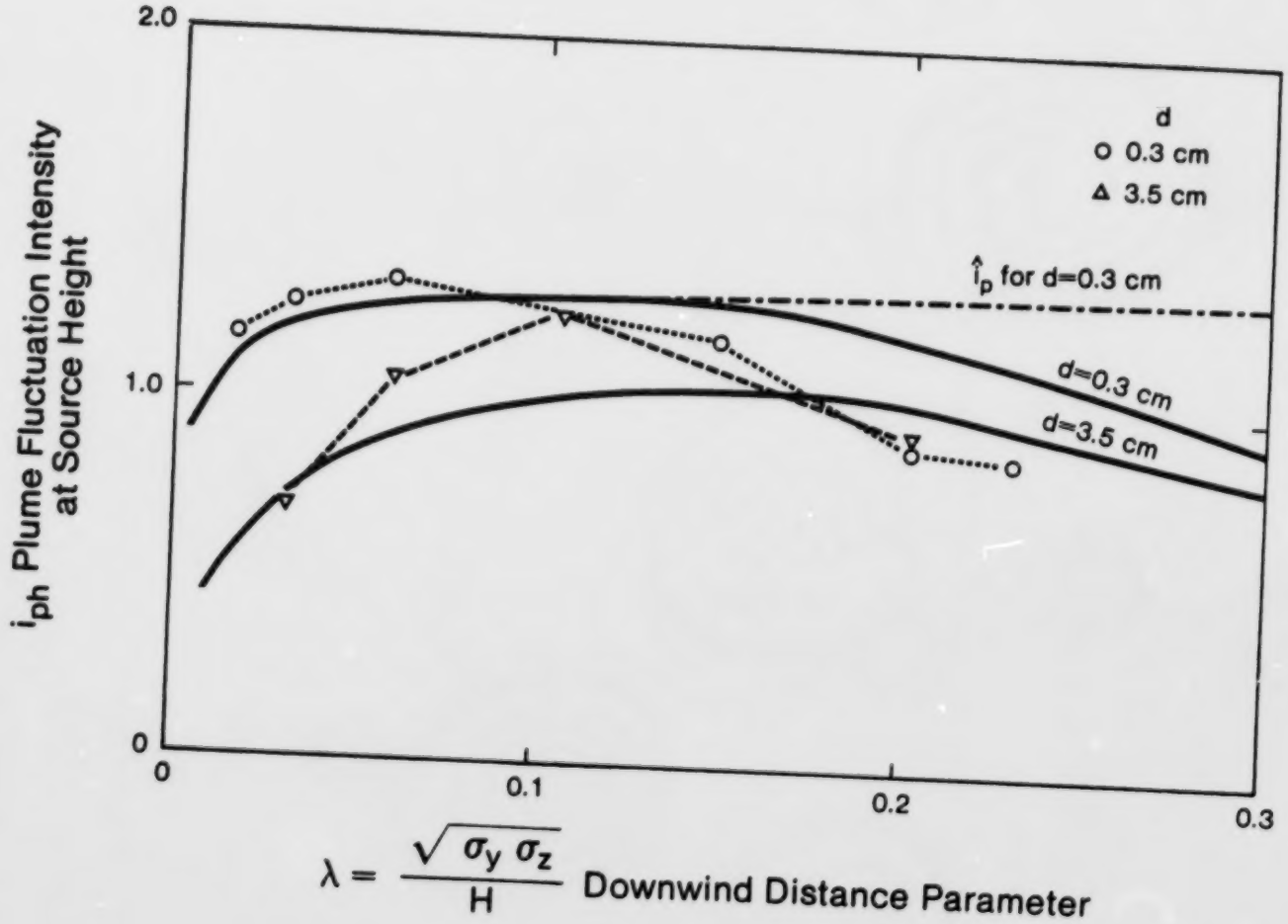

Figure 3-3 Inertial subrange theory for along-wind variation of conditional concentration fluctuation intensity on plume axis for an elevated source in a wind tunnel boundary layer. Data from Wilson, Robins and Fackrell (1985) theory from (3-19), (3-20) and (3-13), (3-14), (3-15) with $\alpha = 0.6$ and $\phi_z = 0.706$

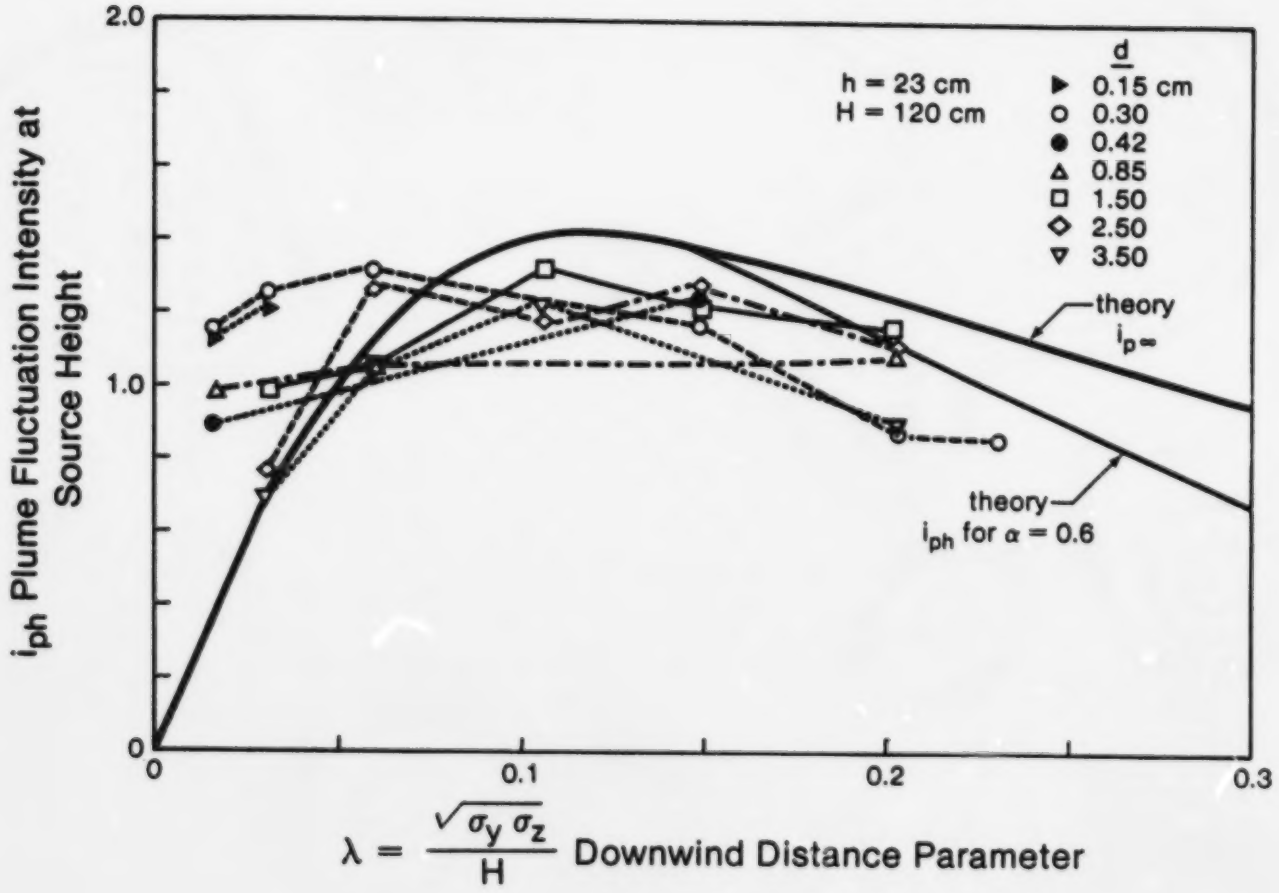

Figure 3-4 Semi-empirical theory for along-wind variation of conditional concentration fluctuation intensity on plume axis for an elevated source in a wind tunnel boundary layer, from Wilson, Robins and Fackrell (1985). Theory from (3-18) and (3-13), (3-14), (3-15) with $\alpha = 0.6$, $\phi_z = 0.706$

$$d_{eff} = d_s \left(\frac{\rho_s}{\rho_a}\right)^{0.5} \frac{W_s}{U_h} \qquad (3\text{-}21)$$

The diameter d_s is the diameter of the "source" jet after any compressible sudden expansion needed to adjust the exit pressure to atmospheric pressure. This expansion process is discussed by Wilson (1981b) p. 19, who showed that for a pipe exit pressure P_e greater than about five times the atmospheric pressure P_a that

$$\frac{d_s}{d} = \left[\frac{1}{2k} \frac{P_e}{P_a}\right]^{0.5} \qquad (3\text{-}22)$$

where d is the actual exit diameter ($d = 2R_e$ on Figure 4-1) and k is the specific heat ratio; $k = 1.4$ for air.

The diameter d_{eff} calculated for (3-21) is used instead of the isokinetic diameter d in (3-11) or (3-20) to compute the virtual origin terms λ_s and λ_{sp} for concentration fluctuations. For a high pressure release from a pipeline rupture the difference between d and d_{eff} can be large. Using Wilson (1981b) for $P_e/P_a = 10$, $d_s = 2d$ in (3-22), and with W_s/U_h typically 100 or greater, from (3-21) we find $d_{eff} = 200\ d$, which is certainly a significant correction.

Summary

A new model for along-wind development of concentration fluctuation intensity has been proposed, based on diffusion in the -5/3 inertial subrange of the turbulence spectrum. The model accounts explicitly for source size effects rather than relying on a purely empirical formulation. Although it is somewhat less accurate than the purely empirical correlation in predicting peak intensities, it produces more realistic values close to and far from the source.

CHAPTER 4

DILUTION CAUSED BY SELF-GENERATED PLUME TURBULENCE

The high velocity jet from a pipe rupture undergoes three different stages of dilution, as shown in Figure 4-1. At the pipe exit the flow is choked at Mach number of unity. Immediately outside the exit the high pressure jet expands to reach pressure equilibrium with the atmosphere. During this rapid expansion phase the following analysis assumes that there is no entrainment of ambient air by the jet. Following the jet expansion the three phase of dilution are:

1) The high velocity jet entrains air by self generated jet turbulence. The entrained air slows the jet until it can bent over by the wind.
2) The bent over jet continues to entrain air as it rises, and counter-rotating vortices are induced by the process of bending over. This rise of the bent over plume is perpendicular rather than parallel to its axis, and this enhances the rate of ambient air entrainment into the plume.
3) The plume reaches its final rise height, and further dilution continues by the process of turbulent diffusion, caused by atmospheric turbulence.

In the following sections, we will make estimates of the dilution caused by self-generated turbulence in the high velocity source jet and the rising bent over plume, and show how they can be superposed on dilution from atmospheric turbulence.

Dilution by Self-Generated Turbulence in the Exhaust Jet

For an incompressible jet the pressure P_e at the pipe exit will be in equilibrium with the atmospheric pressure P_a. The sudden expansion from R_e to R_s

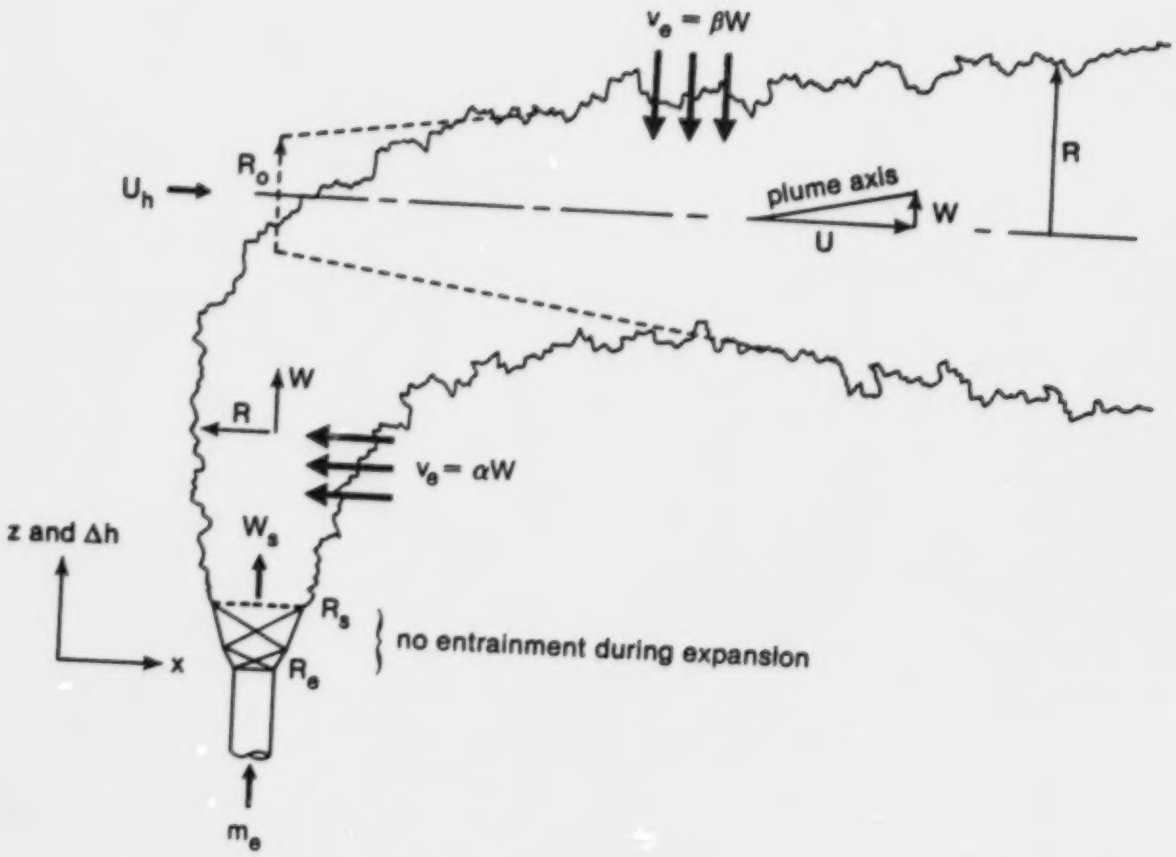

Figure 4-1 Expansion and entrainment into a bent-over buoyant jet from a high pressure pipe release

shown in Figure 4-1 will not occur in incompressible flow, so that $A_e = A_s$ and $\rho_e = \rho_s$ can be used in the general compressible jet dilution equation (C7), which is

$$\frac{\dot{m}}{\dot{m}_e} = 1 + 2\alpha \left(\frac{\rho_a}{\rho_s}\right)^{0.5} \frac{z}{R_s} \qquad (4\text{-}1)$$

where z is the travel distance, R_s is the radius, and α is the jet entrainment constant. The most suprising characteristic of (4-1) is that the jet velocity W_s has no effect on the mass flow dilution ratio.

A pipeline rupture sometimes produces a horizontal jet which is bounded by the ground surface on its lower side, resulting in a half-conical jet. However, because the change in geometry affects both the entrainment in equation (C2) and the momentum conservation in (C4) in the same way, there is no change in the dilution equation (C7), or (4-1) for this situation, except to transform the vertical travel distance z to horizontal distance, x.

For variable density jets the direct entrainment measurements of Ricou and Spalding (1961) yield an entrainment constant $\alpha = 0.08$. Another careful set of measurements by Crow and Champagne (1971) integrated measured velocity profiles at varying downwind distances and obtained $\alpha = 0.073$. Most investigators report values of α that range from 0.08 to 0.11. A value of $\alpha = 0.08$ is a good estimate for a jet in completely calm conditions. However, even a small crosswind velocity U causes a significant increase in entrainment, and a value of $\alpha = 0.10$ is recommended for jets discharging into a crosswind.

After the vertical jet is bent over by the wind it will be carried along at the wind speed U_h rather than its vertical velocity W. At the same time, its rate of entrainment will increase because the rise velocity W is perpendicular to the bent-over jet axis, as shown in Figure 4-1. We account for this by an

enhanced entrainment constant β, which is 4 to 8 times larger than α. The mass flow dilution ratio for a bent-over plume is given by (C16)

$$\frac{\dot{m}}{\dot{m}_e} = \left[1 + \beta \left(\frac{\rho_a}{\rho_e}\right)^{0.5} \left(\frac{U_h}{W_e}\right)^{0.5} \frac{\Delta h}{R_e} \right]^2 \qquad (4\text{-}2)$$

Because there is no entrainment during the sudden expansion, the mass flow at the pipe exit, and at the expanded source shown in Figure 4-1 are the same, so $\rho_s W_s R_s^2 = \rho_e W_e R_e^2$, and (4-2) may be written in terms of the atmospheric pressure source variables as

$$\frac{\dot{m}}{\dot{m}_e} = \left[1 + \beta \left(\frac{\rho_a}{\rho_s}\right)^{0.5} \left(\frac{U_h}{W_s}\right)^{0.5} \frac{\Delta h}{R_s} \right]^2 \qquad (4\text{-}3)$$

Appendix C also develops equations for the mass flow dilution factors for an underexpanded high pressure release from a pipeline rupture or pressure vessel vent. For the common situation where the exit pressure P_e is 10 times or more higher than atmospheric pressure P_a, the mass dilution ratios are given by (C22) for a jet and (C29) for a bent-over plume.

Dilution Factors for Contaminant Concentrations

The concentration of a toxic or flammable component in the gas released from a rupture or exhaust vent is usually expressed as a volume fraction C_e or mass fraction f_e at the pipe exit. These volume and mass fractions at the exit are, for mixtures of ideal gases, equal to the values C_1 and f_1 inside the pipeline.

As the gas in the jet from the pipe exit entrains ambient air, its average molecular weight changes from that of the pipe gas A_e to that of air A_a. At the

same time the mass and volume fractions of contaminant decreases from f_e and C_e to f and C as exhaust gas is diluted. The concentration dilution factors are related to the mass flow dilution factor $\dot{m}/\dot{m}_e$ in Appendix C. If we are far enough from the pipe exit so that entrainment has diluted the exhaust gas to an average molecular weight close to air, the mass fraction dilution factor is given by (C30)

$$\frac{f_e}{f} = \frac{\dot{m}}{\dot{m}_e} \tag{4-4}$$

and the volume fraction dilution factor by (C33)

$$\frac{C_e}{C} = \frac{A_e}{A_a}\left[\left(\frac{\dot{m}}{\dot{m}_e}\right)\right] \tag{4-5}$$

The mass flow ratios may be computed from (4-1) or (4-2) for vertical jets or bent-over plumes. In Appendix C, specific equations are derived for the volume fraction dilution C_e/C from a high pressure compressible gas released as a vertical jet (C35), and a bent-over plume (C34).

Transition from Vertical Jet to Bent-Over Plume Behavior

The fundamental problem with transition from vertical jet dilution in (4-1) to bent-over plume dilution in (4-2) is that the so-called entrainment "constants" α and β are not really constants. In a real plume (see Figure 4-1) the entrainment "constant" increases smoothly from $\alpha \approx 0.08$ near the pipe exit to $\beta \approx 0.6$ as the plume bends over and changes its entrainment characteristics. Because (4-1) and (4-2) were derived from the assumption of constant values of α and β, it is a mathematical form of self-delusion to insert variable

functions for α and β to force the predictions of (4-1) and (4-2) to blend smoothly during transition.

At what point should we switch from the jet dilution of (4-1) to the bent-over plume dilution of (4-2)? Because our interest is in predicting ground level concentrations of toxic gas, we need only concern ourselves with the bent-over plume. It is reasonable to assume that the increased entrainment constant β, and dilution predicted by (4-2), will apply once the plume has been bent over to a 45° angle. As shown in Appendix C, this will occur when

$$\left.\frac{\Delta h}{R_s}\right|_{\text{transition}} = \frac{1}{2\alpha}\left(\frac{\rho_s}{\rho_a}\right)^{1/2}\frac{W_s}{U_h} \tag{4-6}$$

which is (C39) with $z = \Delta h$, the plume rise. The jet dilution equation (4-1) will apply for plume rises smaller than the transition value in (4-6), while the bent-over plume dilution of (4-2) is used for larger rises. It should be kept in mind that the dilution predicted by (4-1) for a jet and (4-2) for a bent-over plume will not be equal at the point of transition.

How diluted is the plume once it begins to bend over? This can be estimated using the transition condition (4-6) in (4-3), to show

$$\left.\frac{\dot{m}}{\dot{m}_e}\right|_{\text{transition}} \simeq \left[1 + \left(\frac{\beta}{2\alpha}\right)\left(\frac{W_s}{U_h}\right)^{0.5}\right]^2 \tag{4-7}$$

For high pressure ruptures, $W_s/U_h > 10$ is a safe assumption, and with $\alpha = 0.1$ and $\beta = 0.6$, (4-6) predicts that the mass flow dilution will always be greater than 100 as the plume enters its bent over phase. It is clear that self-generated turbulence provides considerable dilution near the source.

Combined Dilution from Self-Generated and Atmospheric Turbulence

It is essential that our methods for estimating dilution by self-generated turbulence produce a smooth transition to the dilution predicted by the atmospheric turbulence dispersion model. This Gaussian dispersion equation gives the plume centerline concentration as

$$C_o = \frac{Q}{2\pi\, U_h\, \sigma_y \sigma_z} \tag{4-8}$$

in the absence of ground surface reflection.

The problem is to relate this Gaussian plume model with spreads σ_y and σ_z to the uniform concentration profile of radius R used in plume growth from self-generated turbulence. Wilson (1979) suggests that for the conical plume from self-generated turbulence that the plume radius is

$$R = 2\, \sigma_{self} \tag{4-9}$$

It is easy to show that this radius implies a uniform concentration of $0.5\, C_o$ across the top-hat plume profile to have the same contaminant flow rate Q as the Gaussian in (4-8). Using (C10) for $R = R_o + \beta\Delta h$, and (C15) to estimate the effective initial radius R_o of the bent over plume we find from (4-9)

$$\sigma_{self} = \left(\frac{\rho_e}{\rho_a}\frac{W_e}{U_h}\right)^{0.5} \frac{R_e}{2} + \frac{\beta\Delta h}{2} \tag{4-10}$$

Typically the pipe radius R_e is small, and $W_e/U_h \approx 100$ for high pressure sonic flow at the exit. In this case the initial radius $R_o \approx 5\, R_e$ which is negligible compared to the $\beta\Delta h/2$ term. The self-generated spread becomes

$$\sigma_{self} \approx \frac{\beta\Delta h}{2} \tag{4-11}$$

as suggested by Wilson (1979). Then, assuming that the self-generated turbulence is completely uncorrelated with atmospheric turbulence, the spreading variances simply add, and

$$\sigma_{zc} = (\sigma_z^2 + \sigma_{self}^2)^{0.5} \tag{4-12}$$

where σ_{zc} is the combined atmospheric and self-generated spread.

How important is the spread from self-generated turbulence? For ground level concentrations from high stacks, σ_{self} is always negligible compared to σ_z. However, for a ground level source the situation might be different. For the special case where σ_{yc}/σ_{zc} is a constant, the maximum ground level concentration in a Gaussian plume from a ground level source occurs when

$$\sigma_{zc}^2 = \frac{\Delta h^2}{2} \tag{4-13}$$

Using (4-11) in (4-12) and then equating this to (4-13) leads to

$$\frac{\sigma_{self}}{\sigma_z} = \left[\frac{\beta^2}{2-\beta^2}\right]^{0.5} \tag{4-14}$$

at the point of maximum ground level concentration. For $\beta = 0.6$ we find that $\sigma_{self} = 0.47\ \sigma_z$ and that $\sigma_{zc} = 1.1\ \sigma_z$. This is only a 10% increase, and given the high level of uncertainty in estimating σ_z in the atmosphere, σ_{self} can also be neglected for ground level sources with plume rise.

Because the magnitude of this ground level maximum concentration is proportional to the ratio σ_{zc}/σ_{yc}, the self-generated spread σ_{self} will have a negligible effect because it increases both σ_{yc} and σ_{zc}. From this, we conclude that self-generated turbulence within the plume is unlikely to make any significant contribution to the location of maximum ground level concentration,

or to its magnitude. In contrast, self-generated spread is the major factor contributing to plume dilution during its initial vertical jet and bent over phases, as shown by (4-7).

CHAPTER 5

MOMENTUM AND BUOYANCY CONTRIBUTIONS TO FINAL PLUME RISE

Accidental releases of toxic and flammable gases often occur as high velocity jets from pressure vessels and pipelines. They differ from stack gas emissions in two important ways: jet momentum makes a significant contribution to the trajectory and to the final rise height of these plumes, and secondly, these releases often occur close to ground level and pass through the varying windspeed and turbulence of the surface boundary layer. These differences require changes in the way plume rise is evaluated, in particular, the way in which the effects of momentum and buoyancy are superposed to determine combined rise.

Briggs (1975) presents a solution for plume rise for the case where the entrainment "constant" β is a true constant with downwind distance. For a plume with an initially small diameter at the point of release, the plume rise during this phase, where self-generated turbulence determines the rate of entrainment of ambient air,

$$\Delta h = (\Delta h_M^3 + \Delta h_M^3)^{1/3} \qquad (5\text{-}1)$$

That is, that the contributions of momentum and buoyancy add as a sum of cubes in the transitional rise phase.

To predict final plume rise Wilson (1981) suggested that the sum of cubes law be used as an approximate way of combining the final rises predicted for the separate momentum and buoyancy components. This approach is only an approximation because in the actual combined momentum-buoyancy plume there is a single downwind location that corresponds to final rise, while in the approximation downwind distances to final momentum rise and final buoyancy rise are generally

different. The sum of cubes law in (5-1) is only strictly valid for rise components at the same downwind location, and not for separate components treated as individual plumes with different downwind distances to final rise.

In this chapter we will examine the errors associated with using this sum of cubes law as an approximation for combining the separate momentum and buoyancy contributions to final rise. Because the errors in the approximation depend on the theoretical model chosen to predict the point of final rise, it is worthwhile to first review some of the available physical and theoretical models for this process.

Factors Determining Final Plume Rise

In a stable atmosphere, the approach to final rise is a well understood process. A stable atmospheric temperature variation with height produces a downward force on the rising plume which eventually causes it to level off at its final rise height. In an unstable or neutrally stable atmosphere this restoring force is absent, and because momentum and buoyancy fluxes are conserved, the plume should continue to rise indefinitely as it is carried downwind. However, when the atmosphere is turbulent, plumes tend to level out at a final rise height regardless of atmospheric stability. While it is clear that some interaction occurs between the plume and the atmospheric turbulence which produces this final rise, there is no general agreement as to the physical mechanism by which this occurs. There appear to be three distinctly different schools of thought on the process which leads to final rise. These three physical models are:

1. Atmospheric turbulence gradually modifies the entrainment constant, causing β to increase with downwind distance. The plume rise never actually terminates, but the very large entrainment constant β causes the rate of rise to be negligibly small far

downwind. This approach was used by Bosanquet, Carey and Halton (1950), Bosanquet (1957), Briggs (1969) and Slawson and Csanady (1967), (1971).

2. Atmospheric turbulence causes an "extrainment" of material from the "dynamic" plume. This extrained fluid ceases to assist the plume in rising as a coherent entity. Extrainment is a gradual process which eventually completely depletes the plume of "active" or "dynamic" buoyancy and momentum flux, and leads to a leveling off at final rise. The use of extrainment to deplete the plume of buoyancy and vertical momentum has been used in models proposed by Priestly (1956), Turner (1963), Benjamin (1975) and Netterville (1983).

3. Atmospheric turbulence has little effect on the entrainment process until some critical point is reached where the velocity scale of internal, self-generated plume turbulence becomes less than the equivalent atmospheric turbulence velocity scale. At that point, atmospheric turbulence "breaks up" the plume into uncorrelated parcels which cease to rise in an organized way. This simple model in which the transitional rise is unaffected by atmospheric turbulence, and plume break-up occurs so rapidly that there is a negligible transition distance between transitional and final rise, has been used by Scorer (1959) and by Briggs (1975).

Briggs (1969), (1975) presents a considerable amount of experimental evidence to show that buoyant plumes follow the transitional rise law given in (5-1) over a large portion of their trajectory. For this reason the simple concept of unimpaired transitional rise followed by rapid plume breakup is a useful one for predicting both trajectory and final rise height. In the following section a new model for final rise based on local velocity scales within the inertial subrange of the atmospheric turbulent spectrum will be developed. We will show that this model is equivalent to Briggs approach of defining a characteristic velocity scale by equating the rate of dissipation of internal self-generated plume turbulence to that of the atmospheric turbulence.

Plume Breakup Criteria From Local Spectral Scaling

Before we propose a new criteria for the point of plume breakup and final rise let's look at the existing models of Scorer and Briggs. Scorer (1959) made

the simple assumption that plume breakup occurs at the point where the RMS atmospheric turbulence intensity u' was equal to the average rise velocity W of the plume. In the surface layer of the atmosphere where the RMS intensity u' remains constant with height, Scorer's model leads to a final buoyant rise given by

$$\Delta\tilde{h}_{Bf} \propto \frac{F}{U_h^3} \tag{5-2}$$

Scorer's model is unrealistic because it assumes that all of the atmospheric turbulence energy contributes to plume breakup. For a real plume, the large scale atmospheric turbulence acts only to cause plume meandering but does not break up the organized motions that contribute to plume rise. The atmospheric turbulence eddies which break up the plume must have a scale about the same size as the plume itself, characterized by its radius R.

Briggs (1975) accounted for the scales of atmospheric and plume turbulence by comparing the plume's inertial subrange turbulence with that of the atmosphere. By considering only the inertial subrange, large scale motions that contribute to meandering were effectively excluded. The turbulence spectrum in the inertial subrange is characterized by the rate of energy transfer which is equal to ε, the turbulence dissipation. Using this, Briggs set the point of plume breakup at the location where the dissipation rate of internal self-generated turbulence within the plume, $\bar{\varepsilon}$ equal to the atmospheric dissipation ε. Briggs' criteria for equality of dissipation rates at final rise is discussed in detail in Appendix D where the final rise of a purely buoyant plume is given in (D17) and (D28) which for $\varepsilon = u_*^3/\kappa z$ and the friction velocity u_* proportional to the windspeed U, leads to

$$\tilde{\Delta h}_{Bf} \propto \frac{F}{U_h^3}\left[1 + \frac{h_s}{\tilde{\Delta h}_{Bf}}\right]^{2/5} \tag{5-3}$$

this is identical to (5-2) for a ground level release into the roughness generated turbulence of the surface layer. At the other extreme,

$$\tilde{\Delta h}_{Bf} \propto \frac{F^{3/5}}{U_h^{9/5}} \tag{5-4}$$

for high stacks with small plume rise, in which case the atmospheric dissipation has an approximately constant value of $\epsilon \approx u_*^3/\kappa h_s$ through the plume layer. It is interesting to note that neither of these final rise predictions correspond to

$$\tilde{\Delta h}_{Bf} \propto \frac{F^{3/5}}{U_h} \tag{5-5}$$

developed by Briggs (1969) and currently recommended by Alberta Environment for stack design.

The major difficulty with Briggs approach is a conceptual one. It is difficult to visualize the physical processes involved in breakup when the turbulence energy dissipation rate is used as the governing parameter. The basic concept of rapid plume breakup begins by assuming that the plume radius is initially small, and, because there is little turbulence energy in atmospheric scales of this size the plume growth is dominated by self-generated turbulence. As the plume rises and entrains ambient air its rise velocity and its internal turbulence velocity scale both decrease, and its length scale of turbulence increases in proportion to R, the plume radius. After the plume has grown to sufficiently large size, atmospheric eddies of scale R have the same turbulence energy as self-generated plume turbulence. However, because these entrained

eddies have motions that are uncorrelated with the plume turbulence they cause the plume eddies to lose their correlation, and the organized rising motion of the plume breaks up.

A limiting condition for plume breakup that is physically more satisfying than Briggs' equality of dissipation rates is to equate the turbulence energy w'^2_p of self generated plume turbulence to the turbulence energy w'^2_k of that part of the atmospheric spectrum that has the same length scale of turbulence ℓ_k as the plume. The subscript "k" denotes the energy and scale at a particular wavenumber k in the spectrum. (The wavenumber k is a normalized fluctuation frequency which is inversely proportional to the wavelength of the turbulence). Our assumption is that plume breakup occurs when

$$w'^2_p = w'^2_k \tag{5-6}$$

Using the principle of local scaling of the turbulence spectrum developed in Appendix A as (A13) and (A14) we can write the RMS velocities at turbulence scale ℓ_k as

$$w'_k = \left[\frac{\varepsilon \ell_k}{A_4}\right]^{1/3} \tag{5-7}$$

where A_4 is a constant and ε is the turbulence dissipation rate. In the same way, for the internally generated plume turbulence with its dissipation rate $\bar{\varepsilon}$ and scale ℓ_p

$$w'_p = \left[\frac{\bar{\varepsilon} \ell_p}{A_4}\right]^{1/3} \tag{5-8}$$

The relevant part of the atmospheric turbulence spectrum that influences breakup will have the same scale as the plume turbulence. Setting $\ell_k = \ell_p = R$, the

plume radius, in (5-7) and (5-8) and inserting these in (5-6) results in a plume breakup condition of

$$\bar{\varepsilon}^{2/3} = \varepsilon^{2/3} \tag{5-9}$$

This is exactly the same as Briggs' dissipation condition, except that it is less sensitive to a mismatch in dissipation because for equal energy, dissipation ε appears to the 2/3 power.

The use of local spectral scaling for plume dissipation ε is discussed in Appendix D where it is shown that Briggs' empirical constant η in $\bar{\varepsilon} = \eta\, W^3/\Delta h$ can be derived from other known constants related to the turbulence spectrum. The good agreement between the derived value of $\eta = 1.33$ and Briggs' empirical value of $\eta = 1.5$ is further evidence for the validity of local spectral scaling to define plume turbulence velocity and length scales.

Sum of Cubes Approximation to Final Rise

The final rise height of a plume with combined momentum and buoyancy can be determined exactly by using the sum of cubes law in (5-1). The contributions from momentum and buoyancy are evaluated from (D31) and (D32) in Appendix D, with the time of travel set at t_f, the final rise time from (D25) or (D28). The theory for determining the final rise time using Briggs dissipation criteria for plume breakup is developed in Appendix D.

With an exact expression for final rise in (5-1), why bother developing an approximation? The answer lies in the functional form for the final rise time t_f given in its general form in (D11) and for specific vertical variations of atmospheric dissipation in (D25) and (D28). These functional forms for the final rise time must be solved by iteration, which precludes any simple closed form solution for the relative contributions of buoyancy and the momentum.

It is simpler and physically more satisifying to compute the final buoyancy and momentum rises separately and combine them in some way to determine the final rise. Because the separate final rises occur at different travel times, a sum of cubes of separate final rises similar to (5-1) is only an approximation to the actual final rise. The nature of this approximation is easiest to see by looking at the travel time to final rise of a purely buoyant plume, a momentum jet, and a combined momentum-buoyant plume. In the combined plume both momentum and buoyancy contribute to the production of self-generated turbulence. The turbulence energy and dissipation rate within this combined plume will always be larger than for a purely buoyant plume or a pure momentum jet. The larger turbulence energy in the combined plume allows it to resist breakup by atmospheric turbulence for a greater time of travel. From this we see that the time of travel to final rise of a combined plume will always be larger than the momentum jet component or the buoyant plume component.

However, from a practical point of view, the relevant question is how accurate a sum of cubes of separate final rises is as an approximation to the combined final rise of (5-1). This approximation is discussed in detail in Appendix D where the approximate sum of cubes of separate final rises is written as

$$\Delta\tilde{h}_f = (\Delta\tilde{h}_{Mf}^{\,3} + \Delta\tilde{h}_{Bf}^{\,3})^{1/3} \qquad (5\text{-}10)$$

where the overbar " ~" indicates the separate final rises of the momentum jet and buoyant plume components, and $\Delta\tilde{h}_f$ is the sum of cubes of separate rises.

The separate momentum and buoyancy final rises $\Delta\tilde{h}_{Mf}$ and $\Delta\tilde{h}_{Bf}$ are derived in Appendix D as (D16) and (D17) with (D21) for constant dissipation ε through the plume layer. For a ground level release into roughness generated turbulence the

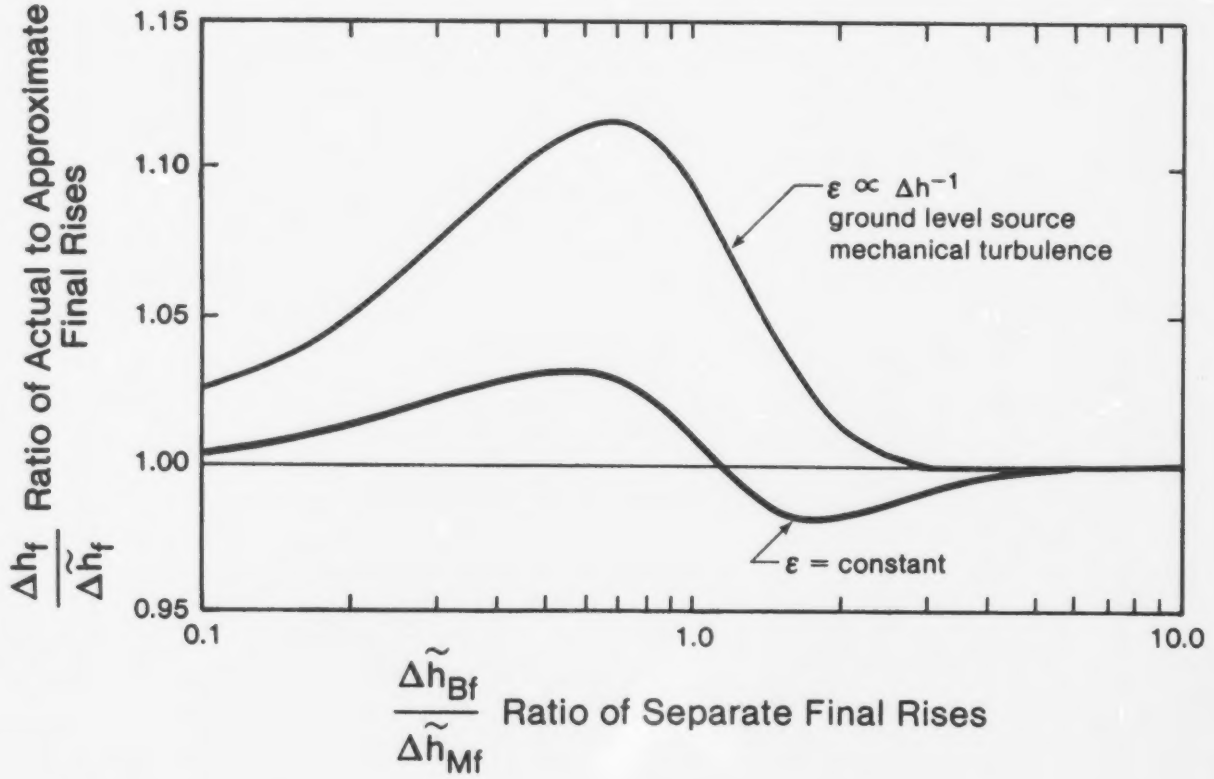

Figure 5-1 Error induced by using sum of cubes law for separate momentum and buoyant final rises instead of combined final rise. Theory from (D25), (D35) and (D28), (D36).

momentum and buoyancy rises are given by (D16) and (D17) with (D22) for the dissipation ε.

The ratio $\Delta h_f/\Delta\tilde{h}_f$ of the exact and approximate final rises in (5-1) at t_f and in (5-12) for separate final rise times $\tilde{t}_{Mf}$ and $\tilde{t}_{Bf}$ is given in Appendix D by (D35) and (D36). This ratio, which represents the error in the "sum of cubes of separate rises" approximation, has the useful characteristic that it can be made a function only of the ratio of buoyant to momentum rises $\Delta h_{Bf}/\Delta h_{Mf}$. In this form it is independent of the entrainment constant β and the self-generated turbulence dissipation rate constant η, both of which must be estimated from experiment.

The ratio of the exact to approximate sum of cubes plume rises from (D25), (D35) and (D28), (D36) are shown in Figure 5-1. The largest errors occur when the final momentum and buoyancy rises are approximately equal. For high stacks, where the atmospheric dissipation is constant through the plume layer, the error is negligible at all buoyancy to momentum rise ratios. For the extreme case of a ground level release into roughness generated surface layer turbulence, the atmospheric dissipation is inversely proportional to the height above ground, see (D19), and errors of about 10% result from the sum of cubes approximation. However, the most important result shown in Figure 5-1 is that the approximation using the sum of cubes of separate final rises will usually underestimate the actual plume rise. This will cause diffusion models to slightly overestimate ground level concentrations, so that the separate rises approximation will err slightly on the conservative side.

APPENDIX A

TOTAL AND INSTANTANEOUS PLUME SPREAD DETERMINED DIRECTLY FROM TURBULENCE PARAMETERS

To estimate the concentration fluctuation intensity for varying sampling times, and at different downwind distances from the source, it is necessary to specify the instantaneous plume widths σ_{iy} and σ_{iz} and the time averaged "total" widths σ_y and σ_z. To be useful for a wide range of atmospheric conditions, these plume widths should be in terms of turbulence length and velocity scales that can be estimated or directly measured. Simple functional forms for σ and σ_i that are consistent with the required asymptotic behavior near to and far from the source will be developed in the following sections.

Total Plume Spread σ_y

To simplify the presentation only the crosswind width σ_y will be considered in detail, and the equivalent results for the vertical spread σ_z written by analogy. The total time averaged plume width σ_y used to estimate the mean concentration c is made up of an instantaneous component σ_{iy}, and a meandering component σ_{my}, which are assumed to be uncorrelated and so have additive variances

$$\sigma_y^2 = \sigma_{iy}^2 + \sigma_{im}^2 \qquad \text{(A1)}$$

A great deal of field and laboratory measurements and analysis exist to estimate this total spread. The measurements suggest that over a very wide range of downwind distances the plume spread follows a power law of the form

$$\sigma_y^2 = \Pi_y^2 x^{2a_y} + \sigma_s^2 \qquad \text{(A2)}$$

The source size σ_s is usually regarded as negligible. Because of the ease with which power law expressions can be used in diffusion analysis, we will propose a model based loosely on Taylor's (1921) statistical theory that preserves this power law form. Assuming that the source size σ_s simply adds in the variance we find, see Csanady (1973) p. 55-56

$$\sigma_y^2 = \left(\frac{v'}{U_c}\right)^2 x^2 + \sigma_s^2 \qquad \text{for } x \ll L_v \tag{A3}$$

and

$$\sigma_y^2 = 2\left(\frac{v'}{U_c}\right)^2 (L_v x - L_v^2) + \sigma_s^2 \qquad \text{for } x \gg L \tag{A4}$$

where v' is the RMS turbulence velocity, U_c is the mean advection speed and L_v is the Lagrangian integral length scale of velocity component v. A simple interpolation equation between the near-source and far downwind limits is given by Snyder (1984) as

$$\sigma_y^2 \approx 2\left(\frac{v'}{U_c}\right)^2 \left(\frac{L_v x^2}{x + 2L_v}\right) + \sigma_s^2 \tag{A5}$$

The advection velocity U_c is related to the travel time t by $U_c = x/t$. In shear flow the advection velocity will in general be different than the local velocity at source height. Some averaging process must be used to define a value of U_c that satisfies mass conservation at each plume cross section.

The Lagrangian length scale L_v is usually estimated from the Eulerian integral scale of turbulence Λ_v. This Eulerian scale is the along-wind correlation of the crosswind turbulence velocity derived from the time series of velocity from a single wind sensor, and the assumption of frozen turbulence. Corsin (1963) suggests a relation of the form

$$L_v = A_1 \frac{\Lambda_v}{(\frac{v'}{U_c})} \qquad (A6)$$

Pasquill (1974) pp. 89-92 reviews the available measurements in the atmospheric boundary layer and finds values of A_1 ranging from 0.35 to 0.80, from which he recommends $A_1 = 0.68 \pm 0.2$. In shear-free grid turbulence Snyder and Lumley (1971) found $A_1 = 1.0$ by direct measurement.

Power Law Approximations

To interpolate between (A3) and (A4) and at the same time maintain a power law functional form like (A2), we assume

$$\sigma_y^2 = (\frac{v'}{U_c})^2 (2L_v)^{2-2a_y} x^{2a_y} + \sigma_s^2 \qquad (A7)$$

where from (A3) and (A7), the exponent a_y must lie somewhere between 1.0 near the source and 0.5 far downwind. By comparing (A2) and (A7) the dimensional constant D_y is

$$D_y = (2A_1\Lambda_v)^{1-a_y} (\frac{v'}{U_c})^{a_y} \qquad (A8)$$

Vertical plume spread σ_y is found in the same way, replacing Λ_v and v' with Λ_w and w'.

One remarkable feature of these power law equations is the wide range of downwind distances over which they apply. Pasquill (1974) p. 228 reviews some experiments that show that crosswind spread follows a power law with $a_y \approx 0.8$ for distances up to a few hundred kilometers. This failure to approach $a_y = 0.5$ for distances larger than about $3L_y$ may be caused by crosswind shear as wind direction changes with height.

Because turbulence scales are much smaller in the vertical, σ_z does have the expected $a_z \approx 0.5$ for $x > 3L_y$, see Pasquill (1974) p. 202. The

process of transition to this asymptotic limit is very gradual, as the growth varies from $\sigma \propto x$ near the source to $\sigma_z \propto x^{0.5}$ far downwind. A power law representation with $a_z \simeq 0.7$ is often a reasonable approximation for distances from 100 m to 5000 m.

Instantaneous Plume Width

The instantaneous plume spread σ_{iy} is needed to estimate the effect of meandering on both mean and fluctuating concentrations. Also, because the spread of an ensemble of instantaneous puffs about their mass centers will be the same as the instantaneous rather than total spread, it is σ_{iy} that is used to characterize puff dispersion.

The essential difference between instantaneous and total plume growth is that different ranges of eddy sizes influence total and instantaneous spread. Neither σ_{iy} or σ_y are significantly changed by eddies much smaller than the instantaneous spread σ_{iy}. Motions of these small eddies are uncorrelated over distances comparable to the instantaneous width. These uncorrelated motions make little contribution to the growth of σ_{iy} or σ_y and act mainly to smear out small scale inhomogenieties within the instantaneous plume. Pasquill (1974) p. 127 demonstrates this effect by spectral analysis of contributions to the total spread σ_y.

Large eddies that cause the instantaneous plume to meander back and forth over a fixed receptor make a contribution to total dispersion σ_y when the sampling time is sufficiently long to include these large time scale motions. In contrast, the instantaneous plume spread σ_{iy} represents the process of relative diffusion about the instantaneous mass center of a plume cross section. This spread is determined by ensemble averaging a large number of instantaneous plume realizations which have each been

shifted to have a common center of mass. Because the effect of meandering by large eddies is removed by considering dispersion relative to the instantaneous mass center, the growth of σ_{iy} is influenced only by eddies about the same size as σ_{iy}. Large eddies act only to push the entire plume around, while the uncorrelated motions of small eddies act mostly to reduce inhomogeniety within the instantaneous plume.

In terms of the spectrum of turbulent velocity fluctuations $E_2(k)$ of v'^2 the process of "total" dispersion that produces σ_y is like a lowpass filter that includes all eddies larger than σ_{iy} in the diffusion process. On the other hand, the relative dispersion that controls σ_{iy} is equivalent to a bandpass filter that includes only narrow ranges of eddy sizes near the plume size σ_{iy}. In the following analysis we will exploit the fact that only the velocity fluctuations near σ_{iy} need to be considered when estimating the instantaneous spread.

It has been observed that the instantaneous spread σ_{iy} is much more sensitive than σ_y to the initial release conditions. Because of this, it is essential to consider the effect of initial source size in developing models for instantaneous width. We will do this by expressing the initial source size as an equivalent virtual spread σ_s.

Estimates of Instantaneous Spread

A quantitative estimate of instantaneous plume spread in relative diffusion was made by Batchelor (1952) and later expanded by Batchelor and Townsend (1956) using dimensional reasoning. Their results apply to turbulence which has an inertial subrange where $E_2(k)$ falls off like $k^{-5/3}$ and can be characterized by a single variable, the kinetic energy

dissipation rate ε. Following Pasquill's (1974) pp. 141-142 review of their results, and using large eddy scaling of dissipation for which $\varepsilon \propto v'^3/\Lambda_v$, they found,

$$\sigma_{iy}^2 = A_2\left(\frac{v'}{U_c}\right)^2\left(\frac{\sigma_s}{\Lambda_v}\right)^{2/3} x^2 + \sigma_s^2 \qquad \text{for } x \ll \Lambda_v \qquad \text{(A9)}$$

very close to the source. The direct dependence of the growth rate on σ_s/Λ_v is due to the source size σ_s setting the initial width of the spectral bandpass filter that determines the fraction of the v'^2 spectrum of that contributes to the instantaneous plume spread. At intermediate distances Batchelor found, for negligible source size

$$\sigma_{iy}^2 = A_3\left(\frac{v'}{U_c}\right)^3 \frac{x^3}{\Lambda_v} \qquad \text{(A10)}$$

This is the accelerated growth phase with $\sigma_i \propto x^{3/2}$ that was observed by Richardson (1926). The value of the constant A_3 can be set using the results of Smith (1968) who applied a Lagrangian analysis of conditioned particle diffusion to show that at intermediate distances

$$\sigma_{iy}^2 = \frac{2}{3}\left(\frac{v'}{U_c}\right)^2 \frac{x^3}{L_v} \qquad x \ll L_v \qquad \text{(A11)}$$

Using (A6) to establish a relation between Eulerian and Lagrangian scales allows (A11) to be written in the same form as (A10) with

$$A_3 = \frac{2}{3A_1} \qquad \text{(A12)}$$

The accelerated growth phase must terminate at some distance because σ_{iy} is always less than σ_y, which is proportional to x^{a_y} with $a_y = 1.0$ near the source and 0.5 far downwind.

Spectral Bandpass Model for Relative Diffusion

In this section we will propose a model for predicting the effect of source size on instantaneous spread and use it to estimate the growth of the instantaneous plume in terms of the turbulence scales and velocities. An added attraction of this model will be the physical insight it provides into the fundamental differences between total and instantaneous dispersion embodied in the spreads σ_y and σ_{iy}.

The essential characteristic of relative diffusion about an instantaneous mass center is that it is the equivalent to imposing a bandpass filter on the turbulent velocity spectrum. Because of this it is only necessary to describe a relatively narrow region of the spectrum that is active in causing instantaneous spread. This frequency band will be $k = \sigma_{iy}^{-1}$, where the wavenumber is the inverse wavelength at frequency n, and is defined as

$$k = \frac{2\pi n}{U_c} = \frac{2\pi}{\text{wavelength}}$$

As σ_{iy} grows larger the frequency band broadens and moves to lower frequencies until eventually the instantaneous plume samples the same frequencies as the total spread, and σ_{iy} is the same as σ_y. In our analysis we assume that the instantaneous plume is small enough that it is influenced only by eddies in the inertial subrange. There is no significant turbulent dissipation or production of v'^2 in this part of the spectrum, so the energy at each frequency depends only by the rate at which energy is transferred from larger to smaller scales. This transfer rate must equal the rate of dissipation ε which ultimately consumes all turbulence kinetic energy after it passes through the inertial subrange. This

dissipation can be estimated from the turbulence kinetic energy v'^2 and the large eddy time scale $t' = \Lambda_v/v'$

$$\varepsilon = A_4 \frac{v'^2}{t'}$$

or

$$\varepsilon = A_4 \frac{v'^3}{\Lambda_v}$$

where $v' = (v^2)^{0.5}$ is the RMS turbulence velocity, Λ_v the integral length scale and A_4 is a constant of order unity.

If the only controlling factor on the spectrum is the rate of energy transfer, then the energy $v_k'^2$ at any wavenumber k must also scale in the same way as (A13), so that

$$\varepsilon = A_4 \frac{v_k'^3}{\ell_k} \tag{A14}$$

where ℓ_k is the length scale of eddies at wavenumber k. Equating (A13) to (A14) gives an estimate of the RMS turbulence at scale ℓ_k as

$$v_k' = v'\left(\frac{\ell_k}{\Lambda_v}\right)^{1/3} \tag{A15}$$

This scaling has been suggested by Sykes, Lewellen and Parker (1984), and will determine the amount of RMS velocity that is effective in causing instantaneous plume spread. Before doing this, it is interesting to see what spectrum shape is implied by (A15). Assuming the local eddy scale ℓ_k at wavenumber k to be

$$\ell_k = \frac{1}{A_5 k} \tag{A16}$$

where A_5 is a constant of order unity. Then writing the definition of spectral density $E_2(k)$ of v'^2

$$\Delta(v_k'^2) = E_2(k)\,\Delta k$$

or

$$E_2(k) = -\frac{\partial(v_k'^2)}{\partial k} \tag{A17}$$

Using (A16) in (A15) and evaluating the spectrum function from (A17) leads to

$$E_2(k) = \frac{2}{3} A_5^{-2/3}\, v'^2\, \Lambda_v^{-2/3}\, k^{-5/3} \tag{A18}$$

Using (A13) to write v'^2 in terms of dissipation ϵ

$$E_2(k) = \frac{2}{3} (A_4 A_5)^{-2/3}\, \epsilon^{2/3}\, k^{-5/3} \tag{A19}$$

which shows that the local velocity scaling of the spectrum assumed in (A14) leads to the expected form for the inertial subrange. The value of the lead constant in (A19) is about 0.74, see Hinze (1975) p. 255. Using the usual value of $A_4 = 0.8$ we find that $A_5 = 1.07$, close to unity.

Effective Eddy Diffusivity for σ_{iy}

To model the growth rate of the instantaneous plume we propose an effective eddy diffusivity K_i. The instantaneous spread is related to the eddy diffusivity by

$$\frac{d\sigma_{iy}^2}{dt} = 2\,K_{iy} \tag{A20}$$

see Csanady (1973) p. 63. Because the instantaneous plume responds only to turbulence scales in the narrow spectral bandpass near σ_{iy}, we assume a turbulent diffusivity

$$K_{iy} = A_6 v_i' \sigma_{iy} \qquad \text{for } \sigma_{iy} < \Lambda_v \tag{A21}$$

where v_i' is the RMS velocity associated with scales of size σ_{iy}. This simple model is limited to the early stages of plume development where $\sigma_{iy} < \Lambda_v$. Once the instantaneous plume grows larger than the integral scale the large eddies will contribute to its growth and it will cease meandering. In the asymptotic limit far downwind from the source, $\sigma_{iy} = \sigma_y$ so that $K_{iy} = K_y$ with

$$K_{iy} = A_7 v' \Lambda_v \qquad \text{for } \sigma_{iy} >> \Lambda_v \tag{A22}$$

Both A_6 and A_7 should be constants of order unity. Using (A22) in (A20), and invoking the Lagrangian-Eulerian relation in (A6) leads to

$$\frac{d\sigma_{iy}^2}{dx} = \frac{A_7}{A_1} \left(\frac{v'}{U_c}\right)^2 L_v \qquad \text{for } \sigma_{iy} >> \Lambda_v$$

where $x = U_c t$ has been used to convert from time of travel to distance coordinates. By differentiating the exact asymptotic solution (A4) with respect to x, it is easy to show that $A_7 = 2 A_1$. With typical values of A_1 ranging from 0.35 to 0.80 the eddy diffusivity constant A_7 is very close to unity, as expected.

In the early stages of plume development meandering causes the instantaneous and total spreads to differ. Using (A21) in (A20) the early growth is given by

$$\frac{d\sigma_{iy}^2}{dt} = 2 A_6 v_i' \sigma_{iy}$$

Expanding the derivative to $2\sigma_{iy} (d\sigma_{iy}/dt)$ gives the growth rate of the instantaneous plume as

$$\frac{d\sigma_{iy}}{dt} = A_6 v_i' \qquad \text{for } \sigma_{iy} < \Lambda_v \tag{A24}$$

with the constant A_6 determined by the width and shape of the spectral bandpass on v' that produces v_i'. With a spectral bandpass centered on a turbulence scale of $\ell_k = \sigma_{iy}$, the effective velocity v_i' from (A15) can be combined with (A24) to write, using $x = U_c t$

$$\frac{d\sigma_{iy}}{dx} = A_6 \frac{v'}{U_c} \left(\frac{\sigma_{iy}}{\Lambda_v}\right)^{1/3} \tag{A25}$$

This equation is restricted by (A24) to $\sigma_{iy} < \Lambda_v$, and by (A15) to the inertial subrange of turbulent spectrum where $\sigma_{iy} << \Lambda_v$. Because the spectrum departs gradually from its inertial subrange form, (A25) becomes progressively less accurate as σ_{iy} approaches Λ_v. For homogeneous turbulence, (A25) can be directly integrated using the initial condition that $\sigma_{iy} = \sigma_s$ at $x = 0$ to obtain

$$\sigma_{iy}^{2/3} = \frac{2}{3} A_6 \left(\frac{v'}{U_c}\right) \frac{x}{\Lambda_v^{1/3}} + \sigma_s^{2/3} \tag{A26}$$

The constant A_6 may be determined by comparing this result to the result of Smith (1968) from (A11) which applies for immediate distances and negligible source size. Using (A6) to relate the Lagrangian scale L_v to the Eulerian scale Λ_v and then equating (A11) to (A26) yields

$$A_6 = \left(\frac{9}{4 A_1}\right)^{1/3} \tag{A27}$$

Measured values of A_1 fall in the range from 0.35 to 0.80, which limits the range of A_6 from 1.4 to 1.9, which meets our expectation of a value near unity. Using (A27) in (A26) gives the final form for the instantaneous spread as

$$\left(\frac{\sigma_{iy}}{\Lambda_v}\right)^2 = \left[\left(\frac{2}{3A_1}\right)^{1/3} \left(\frac{v'}{U_c}\right) \frac{x}{\Lambda_v} + \left(\frac{\sigma_s}{\Lambda_v}\right)^{2/3}\right]^3 \tag{A28}$$

This shows the expected $\sigma^2_{iy} \propto x^3$ region of accelerated growth for $\sigma_s = 0$. However, its most remarkable feature is that source size effects do not simply add as a sum of variances for the instantaneous plume. The form of (A28) increases the downwind distance over which source size has a significant effect on the instantaneous plume width. The source size σ_s contributes 10% of the instantaneous plume width at a distance of

$$\frac{x}{\sigma_s} \simeq 15 \left(\frac{\Lambda_v}{\sigma_s}\right)^{1/3} \frac{U_c}{v'} \qquad \text{(A29)}$$

which for typical atmospheric values of $v'/U_c \simeq 0.10$, $\Lambda_v \simeq 100$ m and $\sigma_s \simeq 2$ m is $x \simeq 1000$ m downwind.

The major deficiency of (A31) is that it assumes that plume spread is always controlled by the inertial subrange, and continues indefinitely at an $x^{3/2}$ growth rate. This form is incorrect far downwind, certainly before $\sigma_{iy} = \Lambda_v$, or when $\sigma_{iy} = \sigma_y$ and all meandering has ceased. However, in atmospheric diffusion this limiting distance may be large, because both Pasquill (1974) p. 228 and Gifford (1977) find no evidence of cloud growth approaching a $\sigma_y \propto x^{0.5}$ asymptote. This suggests that factors such as crosswind shear and non-stationarity cause the apparent length scale Λ_v to increase with plume travel time so that meandering continues to influence plume dispersion at distances up to several hundred kilometers in the atmosphere.

Instantaneous Plume Spread Outside the Inertial Subrange

As the instantaneous plume width increases it will be influenced by large eddies at low frequencies outside the inertial subrange, and this sets the limit of $\sigma_{iy} << \Lambda_v$ on (A29). To extend the spectral bandpass

model further downwind a new form for v_k' is needed. To extend (A15) to the large eddy end of the spectrum, we assume

$$v_k' = v' \left(\frac{\ell_k}{\ell_k + \Lambda_v}\right)^{1/3} \tag{A30}$$

which produces the correct value of $v_k' \to v'$ as $\ell_k \to \infty$. Using the definition of the spectral density $E_2(k)$ in (A17) and scale ℓ_k in (A16), the above equation leads to a spectrum of the form

$$E_2(k) = \frac{2\, A_5 \Lambda_v v'^2}{3(1 + A_5 \Lambda_v k)^{5/3}} \tag{A31}$$

which has the correct integral value

$$v'^2 \equiv \int_0^\infty E_2(k)\, dk \tag{A32}$$

for any value of A_5. The value of A_5 is determined by the zero frequency intercept which must be equal to

$$E_2(0) = \frac{2}{\pi} v'^2 \Lambda_v \tag{A33}$$

which sets the constant at $A_5 = 3/\pi$. With this value, the spectrum produces an inertial range spectrum at high wavenumber of

$$E_2(k) = 0.69\, v'^2 \Lambda_v^{-2/3} k^{-5/3} \tag{A34}$$

The constant 0.69 is in good agreement with measurements in the inertial subrange at high Reynolds number, see Hinze (1975) p. 255. This result leaves us with some confidence in (A30) as a reasonable representation of the spectral bandpass function. Using (A30) in (A24) with a spectral bandpass centered at $\ell_k = \sigma_{iy}$

$$\left(\frac{\sigma_{iy} + \Lambda_v}{\sigma_{iy}}\right)^{1/3} d\sigma_{iy} = A_6\left(\frac{v'}{U_c}\right) dx \tag{A35}$$

To produce a suitable closed form integral we expand the left side of (A35)

$$\left(\frac{\sigma_{iy} + \Lambda_v}{\sigma_{iy}}\right)^{1/3} = \left(\frac{\Lambda_v}{\sigma_{iy}}\right)^{1/3} \left(1 + \frac{\sigma_{iy}}{\Lambda_v}\right)^{1/3} \tag{A36}$$

and approximate the second term to write

$$\left(\frac{\sigma_{iy} + \Lambda_v}{\sigma_{iy}}\right)^{1/3} = \left(\frac{\Lambda_v}{\sigma_{iy}}\right)^{1/3} \left(1 + \frac{1}{4}\left(\frac{\sigma_{iy}}{\Lambda_v}\right)^{2/3}\right) \tag{A37}$$

This approximate form is within 10% of (A36) in the range $0 < \sigma_{iy}/\Lambda_v < 30$. Integrating (A35) using (A37), from σ_s at $x = 0$ to σ_{iy} at x, with A_6 evaluated from (A27)

$$\left(\frac{\sigma_{iy}}{\Lambda_v}\right)^{2/3} + \frac{1}{8}\left(\frac{\sigma_{iy}}{\Lambda_v}\right)^{4/3} = \left(\frac{2}{3A_1}\right)^{1/3} \left(\frac{v'}{U_c}\right) \frac{x}{\Lambda_v} + \Phi_s \tag{A38}$$

with

$$\Phi_s = \left(\frac{\sigma_s}{\Lambda_v}\right)^{2/3} + \frac{1}{8}\left(\frac{\sigma_s}{\Lambda_v}\right)^{4/3} \tag{A39}$$

Equation (A38) is a quadratic with the positive root

$$\left(\frac{\sigma_{iy}}{\Lambda_v}\right)^{2/3} = \left[16 + 8\left(\left(\frac{2}{3A_1}\right)^{1/3} \left(\frac{v'}{U_c}\right) \frac{x}{\Lambda_v} + \Phi_s\right)\right]^{1/2} - 4 \tag{A40}$$

which will be valid for $\sigma_{iy} < \Lambda_v$, a limit imposed by (A24).

APPENDIX B

ALONG-WIND DEVELOPMENT OF CONCENTRATION FLUCTUATIONS

In Wilson, Robins and Fackrell (1982) a model for along wind changes in fluctuation intensity was developed, based on a balance between along-wind advection and dissipation of $\overline{c'^2}$. The effects of source size were dealt with empirically through a virtual origin that depended strongly on source diameter.

The major deficiency of this model was its tendency to underpredict the intensity of fluctuations close to an elevated source. This underprediction is caused by the assusmption that the plume spread parameter

$$\lambda \equiv \frac{(\sigma_y \sigma_z)^{0.5}}{H} \tag{B1}$$

is proportional to $x^{0.5}$. This will only be true very far downwind, and near the source the relation is close to $\lambda \propto x$. In the following analysis we will correct this deficiency, and at the same time make use of a new way of scaling dissipation that accounts explicitly for source size effects.

Using the experimental observation that dissipation and advection are in approximate balance at each point in the plume we have

$$U_c \frac{\partial \overline{c'^2}}{\partial x} = -\varepsilon_c \tag{B2}$$

where U_c is the convection velocity of the plume, and ε_c is the dissipation of concentration fluctuation variance, which we will model through the dissipation time scale T_ε

$$\varepsilon_c = \frac{\overline{c'^2}}{T_\varepsilon} \tag{B3}$$

Assuming that the variance profiles have the self-preserving form

$$\overline{c'^2} = \hat{c}^2 \, g\left(\frac{y}{\sigma_y}, \frac{z}{\sigma_z}\right) \tag{B4}$$

we can combine (B2), (B3) and (B4) and integrate across the plume to obtain

$$U_c \frac{d}{dx}\left[\hat{c}^2 \sigma_y \sigma_z\right] = -\frac{\hat{c}^2 \sigma_y \sigma_z}{T_\varepsilon} \tag{B5}$$

Because source height is not a parameter this result must be limited to plumes with $h \gg \sigma_z$ or, to ground level sources with $h = 0$ for which self-preserving similarity solutions also apply.

The integrated balance equation (B5) was developed from an advection-dissipation balance. Sykes, Lewellen and Parker (1984) developed an exact relation by writing the balance equation for the square $\overline{c^2} = \overline{c}^2 + \overline{c'^2}$. The mean square contains no production terms, and the diffusion terms vanish when integrated over the entire plume. For the special case of Gaussian profiles for both $\overline{c}$ and $\overline{c'^2}$ they obtain, in the appendix to their paper

$$U_c \frac{d}{dx}\left[\left(\hat{c} + \frac{\overline{c}_m^2}{2}\right) \sigma_y \sigma_z\right] = -\frac{\hat{c}^2 \sigma_y \sigma_z}{T_\varepsilon} \tag{B6}$$

where the $\overline{c}_m$ is the spatial average of the mean concentration over the plume cross section (i.e. in y and z). The $\overline{c}_m^2/2$ results from squaring the Gaussian for $\overline{c}$ before integration. Their results show that the $\overline{c}_m^2/2$ term is only important very close to the source, and at all distances of practical interest (B6) produces the same results as (B5).

Modelling the Dissipation Time Scale T_ε

One important contribution of Sykes, Lewellen and Parker (1984) was to suggest a physically realistic model for the dissipation time scale. They suggest that T_ε should be related to the properties that influence the development of the instantaneous plume, rather than the total plume spread which includes meandering. The reasoning behind this is that because meandering acts only to push the entire plume around it does not contribute to dissipation, which is dominated by small scale motions. Using the instantaneous spread σ_i and the RMS turbulence velocity scale u_{si} of eddies of comparable size to the plume we define

$$T_\varepsilon = B_1 \frac{\sigma_i}{u_{si}} \tag{B7}$$

Then, using the spectral scaling developed in Appendix A, the velocity scale of eddies of size σ_i must be related to the total turbulence scale u_s by (A15). For growth in the inertial subrange of the turbulence spectrum

$$u_{si} = u_s\left(\frac{\sigma_i}{\Lambda}\right)^{1/3} \tag{B8}$$

so that (B6) becomes

$$T_\varepsilon = B_1 \frac{\Lambda}{u_s}\left(\frac{\sigma_i}{\Lambda}\right)^{2/3} \tag{B9}$$

Following the turbulent diffusivity model for instantaneous spread from Appendix A, we can express plume spread σ_i in a form similar to (A24)

$$\frac{d\sigma_i}{dx} = B_2 \frac{u_{si}}{U_c} \tag{B10}$$

As shown in Appendix A this equation is valid only for $\sigma_i < \Lambda$. Using (B8), integrate (B10) to obtain equations similar to (A26) and (A28) in Appendix A to obtain

$$\left(\frac{\sigma_i}{\Lambda}\right)^{2/3} = B_2\left(\frac{u_s}{U_c}\right)\frac{x}{\Lambda} + \left(\frac{\sigma_s}{\Lambda}\right)^{2/3} \tag{B11}$$

as suggested by Sykes, Lewellen and Parker (1984). Then, assume the total spread σ, near the source is

$$\frac{d\sigma}{dx} = \frac{u_s}{U_c} \tag{B12}$$

so that

$$\sigma = \frac{u_s x}{U_c} \tag{B13}$$

Here we have made the assumption that the initial source size σ_s has a negligible effect on the total spread, and affects only the instantaneous plume. Combining (B9), (B11) and (B13) we find the dissipation time scale is

$$T_\varepsilon = B_1 \frac{\Lambda}{u_s}\left[B_2\frac{\sigma}{\Lambda} + \left(\frac{\sigma_s}{\Lambda}\right)^{2/3}\right] \tag{B14}$$

Note that the influence of source size is accounted for explicitly by the virtual origin term σ_s/Λ.

At this point we must decide on an appropriate definition for the plume spread σ, and the turbulence scales u_s and Λ. The process of dissipation of $\overline{c'^2}$ is three dimensional in nature and is isotropic in the smallest scales. With this in mind, the form of the integrated balance equation (B5) suggests the form

$$\sigma = (\sigma_y \sigma_z)^{0.5} \tag{B15}$$

With nothing to guide us in our definition of the turbulence length scale Λ, we arbitrarily set

$$\Lambda = \frac{\Lambda_v + \Lambda_w}{2} \tag{B16}$$

By transforming the variance balance equation (B5) from x to σ coordinates, we can avoid the problem of defining the turbulence velocity scale u_s. Using (B12)

$$\frac{d}{dx} = \frac{u_s}{U_c} \frac{d}{d\sigma} \tag{B17}$$

Then with (B17), (B15) and (B14), we can transform (B5) to

$$\frac{d}{dS}\left[\hat{c}^2 S^2\right] = \frac{-B_3 \hat{c}^2 S^2}{(S + S_o)} \tag{B18}$$

where

$$S = \frac{\sigma}{\Lambda}$$

and

$$S_o = B_2^{-1} \left(\frac{\sigma_s}{\Lambda}\right)^{2/3}$$

and

$$B_3 = (B_1 B_2)^{-1}$$

The transformed balance equation may be integrated to obtain

$$\hat{c}^2 S^2 = \frac{B_4}{(S + S_o)^{B_3}} \tag{B19}$$

This can then be normalized by the mean concentration $\bar{c}_o$ on the plume centerline, using a plume mass balance to show that

$$\overline{c}_o S^2 = B_5 \tag{B20}$$

which is constant with downwind distance. Defining another normalized distance as

$$\lambda = \frac{(\sigma_y \sigma_z)^{0.5}}{H} = S \frac{\Lambda}{H} \tag{B21}$$

where H is a convenient constant length scale. In homogeneous turbulence $H \equiv \Lambda$, while in shear flow H may be taken as the shear layer thickness. Using this distance parameter the fluctuation intensity $\hat{i} \equiv \hat{c}/\overline{c}_o$ may be found from the ratio of (B19) to (B20)

$$\hat{i} = B_6 \left(\frac{\Lambda}{H}\right)^{a-1} \frac{\lambda}{(\lambda + \lambda_s)^a} \tag{B22}$$

where $a = B_3/2$, and $B_6 = (B_4/B_5)^{0.5}$. The virtual origin is

$$\lambda_s = B_2^{-1} \left(\frac{\Lambda}{H}\right)^{1/3} \left(\frac{\sigma_s}{H}\right)^{2/3} \tag{B23}$$

By differentiating (B22) it is easy to show that the intensity $\hat{i}$ has a maximum value at $\lambda_{max} = \lambda_s/(a-1)$.

The initial increase of $\hat{i}$ near the source is due to the different decay rates of $\hat{c}$ and $\overline{c}_o$, and not to production of $\overline{c'^2}$ as might seem to be the obvious cause. In fact, production of $\overline{c'^2}$ is neglected in the advection-dissipation balance. Close to the source where $S \ll S_o$ the RMS fluctuation in (B19) decays like $\hat{c} \sim S^{-1}$, while far downwind where $S \gg S_o$, $\hat{c} \sim S^{-(1+a)}$. Because the mean in (B20) $\overline{c}_o \sim S^{-2}$ at all locations, the ratio, $\hat{c}/\overline{c}_o$ will at first increase as $\hat{i} \sim S$ and finally decrease as $\hat{i} \sim S^{1-a}$, even though both $\hat{c}$ and $\overline{c}_o$ decrease continuously.

Equation (B22) for the along-wind development of intensity $\hat{i}$ has an implicit limitation to homogeneous turbulence, where Λ is constant and there are no ground surface dissipation effects. In the next section we will relax the condition of homogeneous turbulence and use (B22) and (B23) for both elevated and ground level sources, where the effective scale Λ must be regarded as a distance dependent average over the plume travel.

Effective Turbulence Scale Λ in Shear Flows

If we consider the limiting cases of a very high source, and a ground level source we find:

- For a high source where $h >> \sigma_z$ the turbulence is approximately homogeneous, and the length scale Λ should be evaluated at $z_{ref} = h$.
- For a ground level source the plume encounters scales which increase with downwind distance as the centroid of the concentration profile increases its distance above the surface. Because Lagrangian similarity theory predicts that both the centroid and the plume spread σ_z increase linearly with time of travel, it is reasonable to evaluate the effective scale Λ at $z_{ref} = B_8\sigma$, where B_8 is a constant.

To interpolate between these limiting cases we define a reference height

$$z_{ref} = \left[h^2 + (B_8\sigma)^2\right]^{0.5} \tag{B24}$$

Finally, assuming a simple linear relation between the effective scale and the reference height

$$\Lambda = B_9\, z_{ref} \tag{B25}$$

Intensity of Conditionally Averaged Fluctuations

The conditionally averaged intensity $\hat{i}_p$ has the intervals of zero concentration removed, and at the same time has no ground surface effects

acting to dissipate fluctuations. To derive a conditional "plume" intensity that is realistic in inhomogeneous turbulence, define $\hat{i}_p$ as the intensity in the distance dependent turbulence experienced by a ground level source, but with no surface dissipation effects. Although this hypothetical case is difficult to simulate experimentally, it may be derived analytically by setting h = 0 in (B24) to find Λ (B25), and using this effective scale in (B22) to obtain

$$i_p = \frac{B_6 \lambda \left(\frac{\Lambda_p}{H}\right)^{a-1}}{[\lambda + \lambda_{sp}]^a} \tag{B26}$$

where from (B24) and (B25) and the definition of λ in (B21)

$$\frac{\Lambda_p}{H} = B_8 B_9 \lambda \tag{B27}$$

and from (B23)

$$\lambda_{sp} = B_2^{-1} \left(\frac{\sigma_s}{H}\right)^{2/3} \left(\frac{\Lambda_p}{H}\right)^{1/3} \tag{B28}$$

This simple method for deducing the conditionally averaged intensity is based on the observation that there is no plume meandering or small scale intermittency on the plume axis for a ground level source. Under these conditions, where diffusion occurs in a field of very small scale turbulence, the conditionally averaged and total plume statistics are identical because the intermittency factor is unity.

APPENDIX C

ENTRAINMENT AND DILUTION BY SELF-GENERATED TURBULENCE

The theory necessary for estimating the dilution in the buoyant jet by turbulence generated within the plume is developed in this Appendix. This self-generated turbulence is caused by the momentum and buoyancy fluxes from the source, and causes entrainment of ambient air into the plume. Close to the source, this self-generated entrainment is the most important mechanism for dilution. As the plume rises and is carried downwind the momentum jet turbulence rapidly decays and buoyancy generated turbulence becomes dominant. Finally, atmospheric turbulence becomes the dominant factor in plume dilution as the decaying buoyancy generated turbulence is overpowered by the constant atmospheric turbulence.

On the following sections the initial dilution in the initial momentum jet will be estimated. Then, the dilution due to combined buoyancy and momentum in the bent over plume will be computed in terms of the plume rise.

Dilution in the Source Jet

To simplify the analysis, assume that the jet has travelled far enough to entrain sufficient air that its density is close to the ambient air density ρ_a. This distance will depend on the composition of the pipe gas, but will be at least as far as the distance to the point where compressibility effects are negligible. Wilson (1981 b) pp. 36-37 showed that this is about $x > 30\ D_e$, where D_e is the source exit diameter.

The experimental results of Ricou and Spalding (1961) showed that the process of air entrainment is kinematic rather than dynamic, so that the entrainment rate depends only on jet velocity and not on its density. The entrainment velocity is defined by

$$v_e = \alpha W \tag{C1}$$

with an entrainment constant α that is independent of densities ρ_a and ρ_e. Because the entrained mass is at density ρ_a, the mass added to the jet in distance dz is

$$\dot{dm} = \rho_a v_e (2\pi R dz) \tag{C2}$$

Using (C1) this can be written

$$\frac{\dot{dm}}{dz} = 2\pi \alpha \rho_a R W \tag{C3}$$

Because both jet velocity and radius vary with distance, a momentum balance must be used to relate R and W. Using the approximation that the local jet density is equal to the ambient air density ρ_a allows us to write the momentum balance in the constant pressure jet, which begins after its initial expansion from "e" to "s", (the "source" condition)

$$\rho_s \pi R_s^2 W_s^2 = \rho_a \pi R^2 W^2 \tag{C4}$$

so that

$$W = \left(\frac{\rho_s}{\rho_a}\right)^{0.5} \frac{R_s}{R} W_s \tag{C5}$$

Because there is no crater drag interaction here, the "source" condition is equivalent to the "expanded jet" condition denoted by a subscript "j" in Wilson (1981 b). Using (C5) in (C3),

$$\frac{\dot{dm}}{dz} = \frac{2\alpha}{R_s} \left(\frac{\rho_a}{\rho_s}\right)^{0.5} \dot{m}_e \tag{C6}$$

where $\dot{m}_e = \dot{m}_s = \rho_s \pi R_s^2 W_s$ is the mass release rate. Integrating this between the origin at "s" and a height z yields the mass dilution ratio

$$\frac{\dot{m}}{\dot{m}_e} = 1 + 2\alpha \left(\frac{\rho_a}{\rho_s}\frac{A_e}{A_s}\right)^{0.5} \frac{z}{R_e} \qquad (C7)$$

The area ratio $A_e/A_s = R_e^2/R_s^2$ has been introduced to allow distance z to be normalized with the actual pipe exit radius R_e rather than the hypothetical source radius R_s.

Dilution in a Rising Bent-Over Plume

Briggs (1975) shows that the transition from a vertical jet to a bent over plume occurs very rapidly, and that most of the trajectory can be approximated as fully bent over, with the plume axis nearly parallel to the wind. As the plume bends over a pair of counter rotating vortices develop which enhance entrainment into the underside of the plume. At the same time, the vertical velocity W moves the bent over plume perpendicular to its axis, causing more entrainment than in a vertical jet. To account for this we define an enhanced entrainment coefficient β,

$$v_e = \beta W \qquad (C8)$$

Spillane (1983) reviews several other entrainment models that can be applied to the transitional bending-over phase. Typically β = 0.4 to 0.8, while the vertical jet entrainment coefficient is only α = 0.08. By the time the jet is bent over, it has entrained enough ambient air that its density is close to ρ_a. Because the convection velocity is a constant U_h, rather than the jet velocity W that varies within z, a mass balance yields

$$\frac{dR}{dz} = \beta \qquad (C9)$$

Defining an effective initial radius R_0 that contains the mass emission rate

$\dot{m}_e$, see Figure 4-1, and integrating (C9) from z = 0 to the plume rise height z = Δh

$$R = R_o + \beta \Delta h \tag{C10}$$

Because the plume has a density ρ_a and is carried along at speed U_h, the initial radius R_o must be related to $\dot{m}_e$ by

$$\dot{m}_e = \rho_a \pi R_o^2 U_h \tag{C11}$$

The total mass flux through a plume cross section is

$$\dot{m} = \rho_a \pi R^2 U_h \tag{C12}$$

Taking the ratio of (C12) to (C11) and using (C10) the mass dilution ratio is

$$\frac{\dot{m}}{\dot{m}_e} = \left(1 + \frac{\beta \Delta h}{R_o}\right)^2 \tag{C13}$$

At the pipe exit the mass flow is

$$\dot{m}_e = \rho_e \pi R_e^2 W \tag{C14}$$

Equating (C11) and (C14) allows the effective radius R_o at the origin to be expressed in terms of the pipe exit radius R_e

$$\frac{R_e}{R_o} = \left(\frac{\rho_a}{\rho_e} \frac{U_h}{W_e}\right)^{0.5} \tag{C15}$$

Using this in (C13) the mass flow in the bent over plume is

$$\frac{\dot{m}}{\dot{m}_e} = \left[1 + \beta \left(\frac{\rho_a}{\rho_e} \frac{U_h}{W_e}\right)^{0.5} \frac{\Delta h}{R_e}\right]^2 \tag{C16}$$

Compare this to the mass dilution for a vertical jet given in (C7). For a jet, the dilution is linear in rise distance, while for a bent over plume it varies

as the square of the plume rise. The more rapid dilution of a bent over plume is due to the constant convection velocity U_h, in contrast to the convection velocity W which decreases with distance in a vertical momentum jet.

High Pressure Pipeline Ruptures

The mass dilution ratios for a vertical jet and a bent over plume in (C7) and (C16) apply to any fluid, as long as the jet is sufficiently diluted to have a density near ambient ρ_a. In this section the flow characteristics and fluid properties of a high pressure choked (i.e. sonic velocity) gas release will be used to express the dilution in terms of the readily available pressure P_e and stagnation temperature T_1 at the pipe exit. From the ideal gas law the density ratio in (C7) is

$$\frac{\rho_a}{\rho_s} = \frac{A_a}{A_e} \cdot \frac{T_s}{T_a} \qquad \text{(C17)}$$

where A is the molecular weight and T the absolute temperature. The molecular weight remains the same during the expansion because no air is entrained. With $A_1 = A_e = A_s$ we will use A_e throughout as the pipe gas molecular weight. For adiabatic flow the jet temperature T_s is

$$\frac{T_1}{T_s} = 1 + \left(\frac{k-1}{2}\right) M_s^2 \qquad \text{(C18)}$$

where M_s is the Mach number in the expanded jet. Wilson (1981b) p. 19 shows that for high pressure at the pipe exit

$$M_s = \left(2(k+1)\right)^{0.5} \qquad \text{(C19)}$$

as long as $P_e/P_a > 10$. Using (C19) in (C18)

$$\frac{T_1}{T_s} \simeq k^2 \tag{C20}$$

Wilson (1981b) p. 19 also showed that even at moderate exit pressure ratios,

$$\frac{A_s}{A_e} \simeq \frac{1}{2k}\left(\frac{P_e}{P_a}\right) \tag{C21}$$

By using (C17), (C20) and (C21) in (C7) the mass dilution ratio for a vertical jet becomes

$$\frac{\dot{m}}{\dot{m}_e} \simeq 1 + 2\,\alpha\, a_1\left(\frac{2}{k}\right)^{0.5}\frac{z}{R_e} \tag{C22}$$

where

$$a_1 \equiv \left[\frac{A_a}{A_e}\left(\frac{T_1}{T_a}\right)\left(\frac{P_a}{P_e}\right)\right]^{0.5} \tag{C23}$$

The approximation in (C22) is limited to high exit pressures $P_e/P_a > 10$ and to distances far enough from the exit that the jet density is approximately equal to that of the ambient air.

Next, consider the equivalent process for a bent-over plume whose mass flow is given by (C16). To evaluate the density ratio and exit velocity in (C16) the choked flow condition of $W_e = s_e$ is used, where s_e is the speed of sound at the pipe exit temperature

$$s_e = \left(\frac{k\,\bar{R}\,T_e}{A_e}\right)^{0.5} \tag{C24}$$

$$= \left(\frac{k\,\bar{R}\,T_1}{A_e}\right)^{0.5}\left(\frac{T_e}{T_1}\right)^{0.5} \tag{C25}$$

The first bracketed term is the speed of sound s_1 in the pipe gas at its stagnation temperature T_1. The temperature ratio in the second term is given by

$$\frac{T_1}{T_e} = 1 + \left(\frac{k-1}{2}\right) M_e^2 \tag{C25}$$

where the Mach number $M_e = 1.0$ in the choked exit flow, so

$$\frac{T_1}{T_e} = \frac{k+1}{2} \tag{C26}$$

Using this in (C24)

$$W_e = s_e = \left(\frac{k+1}{2}\right)^{0.5} s_1 \tag{C27}$$

From the ideal gas law the density ratio in (C16) is:

$$\frac{\rho_a}{\rho_e} = \frac{P_a}{P_e} \frac{A_a}{A_e} \frac{T_e}{T_a} \tag{C28}$$

with (C26) and (C27) this allows us to write (C16)

$$\frac{\dot{m}}{\dot{m}_e} = \left[1 + \beta a_1 \left(\frac{2}{k+1}\right)^{0.25} \left(\frac{U}{s_1}\right)^{0.5} \frac{\Delta h}{R_e} \right]^2 \tag{C29}$$

where the constant a_1 is defined by (C23)

Dilution Factors for Mass and Volume Concentration

The concentration of a toxic or flammable component in a mixture is often expressed in terms of its volume fraction, c. By assuming that this component and the entire mixture both behave as ideal gases we can develop the relationship of volume fraction, c, to the mass fraction f. It is easy to show that the

dilution factor for mass fraction is just the ratio of mass flow rates. That is,

$$\frac{f_e}{f} = \frac{\dot{m}}{\dot{m}_e} \tag{C30}$$

where f is the mass fraction of the component at distance z from the exit, and f_e is the mass fraction of this component in the pipeline gas. This mass fraction dilution factor may be directly determined from (C22) for a jet, or from (C29) for a bent over plume.

The relationship of mass and volume fraction may be found from the ideal gas law. Using the law of partial volumes, the volume fraction c and mass fraction f of a specific component gas are related by

$$c = f \frac{A_{mix}}{A} \tag{C31}$$

where A is the molecular weight of the component and A_{mix} the molecular weight of the mixture.

During the dilution process air is entrained by the jet, changing the molecular weight of the mixture from $A_{mix} = A_e$ at the pipe exit point to $A_{mix} = A_a$ the molecular weight of ambient air. Taking the ratio of the volume fraction c_e in the pipeline gas to the jet concentration, c, at a point far enough from the exit to have a density close to ambient air, we find the volume dilution factor, c_e/c

$$\frac{c_e}{c} = \frac{A_e}{A_a}\left(\frac{f}{1}\right) \tag{C32}$$

Using (C30)

$$\frac{c_e}{c} = \frac{A_e}{A_a}\left(\frac{\dot{m}}{\dot{m}_e}\right) \tag{C33}$$

Combine (C29) and (C33), with (C23) to evaluate the parameter a_1, and we find for a bent over plume

$$\frac{c_e}{c} = \left[\left(\frac{A_e}{A_a}\right)^{0.5} + \beta\left[\frac{T_1}{T_a}\frac{P_a}{P_e}\left(\frac{2}{k+1}\right)^{0.5}\frac{U}{s_1}\right]^{0.5}\frac{\Delta h}{R_e}\right]^2$$

and for a jet, using (C22), (C23) and (C33) the dilution factor is

$$\frac{c_e}{c} = \left[\frac{A_e}{A_a} + 2\alpha\left[\frac{A_e}{A_a}\frac{T_1}{T_a}\frac{P_a}{P_e}\left(\frac{2}{k}\right)\right]^{0.5}\frac{z}{R_e}\right] \tag{C35}$$

It is interesting to note that for a horizontal half-conical jet bounded by the ground, the change in geometry will affect both the entrainment and momentum conservation in (C2) and (C4) in the same way. Because of this, the dilution in a "half jet" will also be given by (C35).

Transition From Vertical Jet to Bent-Over Plume

As the wind bends the vertical jet over, its mass flow rate dilution will gradually change from (C7) to (C16). We will assume that the point of transition where (C16) can be applied occurs when the plume is bent over at an angle of 45°. At this point, the plume trajectory will have a slope of unity. By simple kinematics the vertical velocity W of the jet must equal the windspeed U_h that is bending the plume over. Setting $U_h = W$ in (C5)

$$\frac{R}{R_s} = \left(\frac{\rho_s}{\rho_a}\right)^{0.5}\frac{W_s}{U_h} \tag{36}$$

Wilson (1981b) suggests that density differences will have little effect on jet spreading rate, so that

$$\frac{dR}{dz} = 2\alpha \tag{C37}$$

To simplify the transition condition, assume that the virtual origin of the jet is at the pipe exit. Integrating (C37) using this assumption of $R = 0$ at $z = 0$,

$$R = 2\,\alpha\, z \tag{C38}$$

so that transition to bent-over plume behavior in (C36) occurs when

$$\left.\frac{z}{R_s}\right|_{\text{transition}} > \frac{1}{2\alpha}\left(\frac{\rho_s}{\rho_a}\right)^{0.5}\frac{W_s}{U_h} \tag{C39}$$

This is only an approximate estimate because the point of 45° slope was chosen arbitrarily. Also the entrainment "constant" α increases during the process of bending over, making α in (C39) difficult to define.

APPENDIX D

SUM OF CUBES APPROXIMATION TO FINAL RISE

In this appendix Briggs (1975) plume rise model will be reviewed by presenting the theoretical equations for plume rise due to the combined effects of stack gas buoyancy and vertical jet momentum. Briggs' turbulent dissipation criterion for determining the point of final rise depends on an estimate of the rate of dissipation $\bar{\epsilon}$ within the plume due to its self-generated turbulence. His estimate will be shown to be consistent with the local scaling model developed in Appendix A. The times of travel to the point of final rise of pure momentum jets and pure buoyant plumes, will be compared to the travel time of a combined buoyant jet to its final rise.

The combined momentum and buoyant rise of a plume depends strongly on the rate of entrainment of ambient air into the plume. This is characterized by an entrainment velocity v_e, which for a bent-over plume with its axis close to horizontal is related to the vertical local rise velocity W

$$v_e = \beta W \tag{D1}$$

as shown schematically in Figure 4-1. Briggs (1975) solved the mass, momentum and thermal energy conservation equations for the case where the entrainment "constant" β is independent of x, (but may still be a function of the same source velocity ratio W_s/U_h). In this case the plume rise Δh reduces to the simple closed form

$$\Delta h = \left[\frac{3}{\beta^2} \frac{F_M}{U_h} t + \frac{3}{2\beta^2} \frac{F}{U_h} t^2 \right]^{1/3} \tag{D2}$$

in terms of the plume travel time, t. Equation (D2) also requires a uniform wind speed, constant with z throughout the plume layer from $z = h_s$ to $z = h_s + \Delta h$. This constant wind speed U_h allows the travel time t to be related to downwind distance by $x = U_h t$. The key parameters in (D2) are the momentum and buoyancy fluxes, F_M and F, which are defined as

$$F_M = \left(\frac{\rho_s}{\rho_a}\right) W_s^2 R_s^2 \tag{D3}$$

and

$$F = g \left(\frac{\rho_a - \rho_s}{\rho_a}\right) W_s R_s^2 \tag{D4}$$

Final Rise Using Briggs Criteria

Briggs (1975) assumes that final rise occurs when the average dissipation rate $\bar{\varepsilon}$ of self-generated turbulence energy within the plume is equal to the local atmospheric turbulence dissipation rate $\bar{\varepsilon}$. When these two rates are equal Briggs hypothesizes that the atmospheric turbulence is able to "invade" the plume and decorrelate its mixing processes, causing it to "break up". To make use of this condition to predict final rise, we must first express the internal dissipation rate in terms of plume rise. Using large eddy scaling of turbulent dissipation (see (A13) in Appendix A)

$$\bar{\varepsilon} = A_4 \frac{w_p'^2}{\ell_p} \tag{D5}$$

where w_p' is the root mean square turbulence velocity within the plume, and ℓ_p is the scale of large self-generated eddies within the plume. The constant

$A_4 \approx 0.8$ from experimental measurements of a wide range of turbulent flows. If we make the rather crude estimate that

$$w_p' \approx W \tag{D9}$$

and

$$\ell_p \approx R \tag{D7}$$

where $R = \beta\Delta h$ is the plume radius. We obtain, for $A_4 = 0.8$ and $\beta = 0.6$

$$\varepsilon = 1.33 \frac{W^3}{\Delta h} \tag{D8}$$

Rather than constrain ourselves with this estimate, we will follow Briggs' convention and leave the constant to be determined later as

$$\bar{\varepsilon} = \eta \frac{W^3}{\Delta h} \tag{D9}$$

Briggs (1975) p. 75 estimates that $\eta = 1.5$, which is quite close to the independently computed value of $\eta = 1.33$ in (D8). The time of travel until final rise is found by observing that

$$W = \frac{d(\Delta h)}{dt} \tag{D10}$$

and using the combined rise equation (D2) to evaluate both W and Δh in (D10). Setting internal and external dissipation rates equal at the point where final rise occurs, $\bar{\varepsilon} = \varepsilon$ we find after some manipulation

$$\frac{3}{\beta^2}\frac{F_M}{U_h} t_f + \frac{3}{2\beta^2}\frac{F}{U_h} t_f^2 = \left[\frac{3}{\beta^2}\frac{F_M}{U_h} + \frac{3}{\beta^2}\frac{F}{U_h} t_f\right]^{9/7} \left(\frac{\eta}{27\varepsilon}\right)^{3/7} \tag{D11}$$

where $t_f = x_f/U_h$ is the plume travel time at the point of final rise.

Final Rise of Pure Buoyant Plumes and Momentum Jets

For a pure momentum jet the buoyancy flux F = 0, and (D11) gives the time to final rise as

$$\tilde{t}_{Mf} = \left[\frac{3}{\beta^2}\frac{F_M}{U_h}\right]^{2/7}\left(\frac{\eta}{27\varepsilon}\right)^{3/7} \tag{D12}$$

and a final rise height from (D2) with F = 0 of

$$\Delta\tilde{h}_{Mf} = \left[\frac{3}{\beta^2}\frac{F_M}{U_h}\tilde{t}_{Mf}\right]^{1/3} \tag{D13}$$

The superscript " ~ " indicates a pure momentum jet or buoyant plume. For a pure buoyant plume the momentum flux $F_M = 0$ and from (D11) and (D2) the time to final rise $\tilde{t}_{Bf}$ and the rise height $\Delta\tilde{h}_{Bf}$ are

$$\tilde{t}_{Bf} = 2^{9/5}\left[\frac{3}{2\beta^2}\frac{F}{U_h}\right]^{2/5}\left(\frac{\eta}{27\varepsilon}\right)^{3/5} \tag{D14}$$

and

$$\Delta\tilde{h}_{Bf} = \left[\frac{3}{2\beta^2}\frac{F}{U_h}\tilde{t}_{Bf}^{2}\right]^{1/3} \tag{D15}$$

Inserting (D12) in (D13) and (D14) in (D15) leads to the form given by Briggs (1975)

$$\Delta\tilde{h}_{Mf} = \left[\frac{1}{\beta^2}\frac{F_M}{U_h}\right]^{3/7}\left(\frac{\eta}{\varepsilon}\right)^{1/7} \tag{D16}$$

and for the buoyant plume

$$\Delta\tilde{h}_{Bf} = \left[\frac{2}{3\beta^2}\frac{F}{U_h}\right]^{3/5}\left(\frac{\eta}{\varepsilon}\right)^{2/5} \tag{D17}$$

It is clear from these expressions that variation with height of the atmospheric turbulence dissipation, ε, must be known in order to determine the final rise.

Variation of Atmospheric Dissipation with Height

Most stack designs are based on dispersion in neutral atmospheric stability, where mechanically generated turbulence from wind shear is the only mechanism for dispersion. Neutral stability produces a log-law velocity profile in the surface layer so that

$$U = \frac{u_*}{\kappa} \ln \left(\frac{z}{z_0}\right) \tag{D18}$$

where $\kappa = 0.4$ is von Karman's constant. It can be shown that turbulent dissipation in this log-law surface layer is

$$\varepsilon = \frac{u_*^3}{\kappa z} \tag{D19}$$

At plume height, where $z = (h_s + \Delta h)$ this becomes

$$\varepsilon = \frac{u_*^3}{\kappa(h_s + \Delta h)} \tag{D20}$$

This variation of ε with height leads to closed form solutions for plume rise for the limiting cases of tall stacks and for ground level releases. For tall stacks in high winds, where $h_s \gg \Delta h$ we find

$$\varepsilon = \frac{u_*^3}{\kappa h_s} = \text{CONSTANT} \tag{D21}$$

A constant value of ε with height is also typical of unstable atmospheric mixing where convective turbulence is dominant, at times of strong solar heating of the ground combined with light winds. The approximation for ε in (D21) does not apply, but the general results for constant ε in the following analysis will be valid.

Another case of practical interest is the release from a ground level source into mechanical turbulence. In this case the stack height $h_s = 0$ and turbulence dissipation varies directly with plume rise height Δh,

$$\varepsilon = \frac{u_*^3}{\kappa \, \Delta h} \tag{D22}$$

In the following sections combined rise equations for these limiting cases of ε = constant and $\varepsilon \propto \Delta h^{-1}$ will be developed.

Normalizing Plume Rise Variables to Obtain Parametric Solutions

When the stack height h_s is much larger than the plume rise, or in the convective turbulence, the atmospheric turbulence dissipation ε is almost constant through the plume rise layer. In the first case considered below we will assume that ε is a constant, and use the ratios of plume rise so that ε, the entrainment constant β, and other difficult to determine parameters conveniently cancel.

The ultimate objective of this analysis is to determine the ratio of the actual combined rise of a plume with both momentum and buoyancy to the approximate rise found by considering buoyancy and momentum rise separately and then adding them as a sum of cubes. The only difficulty is that an explicit solution can not be found for this ratio. Instead, several equations are required, connected through a dimensionless momentum flux to buoyancy flux ratio ξ, which is defined as

$$\xi = \frac{2 F \tilde{t}_{Mf}}{F_M} \tag{D23}$$

where F and F_M are the buoyancy and momentum fluxes and $\tilde{t}_{Mf}$ from (D12) is the time to final rise of a pure momentum jet with the same momentum flux and entrainment constant as the buoyant-momentum plume. For the special case where the atmospheric turbulence dissipation ε is a constant with height, the mysterious collection of terms used to define ξ can be directly related to the pure buoyant and momentum final rises in (D16) and (D17) by

$$\xi = \left[\frac{\Delta\tilde{h}_{Bf}}{\Delta\tilde{h}_{Mf}}\right]^{5/3} \qquad \text{for } \varepsilon \equiv \text{CONSTANT} \tag{D24}$$

The time of travel t_f to the point of final rise for the combined plume can be expressed in terms of ξ and the final rise time $\tilde{t}_{Mf}$ of a pure momentum jet by using (D12) and (D23) in (D11) to obtain

$$r_1 = \frac{(1 + \frac{\xi}{2} r_1)^{9/7}}{(1 + \frac{\xi}{4} r_1)} \qquad \text{for } \varepsilon \equiv \text{CONSTANT} \tag{D25}$$

where the time ratio r_1 is defined as

$$r_1 \equiv \frac{t_f}{\tilde{t}_{Mf}} \qquad \text{for } \varepsilon = \text{constant} \tag{D26}$$

Note that (D25) is an implicit equation that must be solved by iteration for each specified value of the rise ratio ξ.

Similar equations can be developed for the case of a ground level release into mechanical turbulence where the atmospheric turbulence dissipation

ε is a function of height, given by (D22). Using (D22) in (D12) to get $\tilde{t}_{Mf}$ and then using this in (D23),

$$\xi = \frac{\Delta\tilde{h}_{Bf}}{\Delta\tilde{h}_{Mf}} \qquad \text{for } \varepsilon \propto (\Delta h)^{-1} \tag{D27}$$

For this case, the parametric variable ξ is simply the ratio of buoyancy to momentum final rise. Then, using (D23) in (D11) and combining (D22) and (D12),

$$r_2 = \frac{(1 + \frac{\xi}{2} r_2)^{3/2}}{(1 + \frac{\xi}{4} r_2)} \qquad \text{for } \varepsilon \propto (\Delta h)^{-1} \tag{D28}$$

where the time ratio r_2 is defined in the same way as r_1

$$r_2 = \frac{t_f}{\tilde{t}_{Mf}} \qquad \text{for } \varepsilon \propto (\Delta h)^{-1} \tag{D29}$$

Now, with the parametric variables ξ, r_1 and r_2 defined, we can derive equations for the ratio of combined final rise to its sum of cubes approximation.

Ratio of Combined Final Rise to "Sum of Cubes of Final Rises" Approximation

The transitional plume rise equation (D2) clearly shows that momentum and buoyancy effects add according to a sum of cubes law. This is easy to see when (D2) is written at the point of final rise

$$\Delta h_f = (\Delta h_{Mf}^3 + \Delta h_{Bf}^3)^{1/3} \tag{D30}$$

where the buoyancy and momentum rise components are, at final rise where the travel time $t = t_f$

$$\Delta h_{Mf} = \left[\frac{3}{\beta^2} \frac{F_M}{U_h} t_f \right]^{1/3} \tag{D31}$$

$$\Delta h_{Bf} = \left[\frac{3}{2\beta^2} \frac{F}{U_h} t_f^2 \right]^{1/3} \tag{D32}$$

with these definitions this sum of cubes law is an exact expression.

A simpler approximate form for the final rise results when we apply the sum of cubes law to the final rises of the momentum jet and buoyant plume components as if they were two separate plumes. These separate plume rises have been designated by a superscript " ~ " in (D16) and (D17) to distinguish them from the actual components of the combined final rise in (31) and (32). Following this notation, the approximate sum of cubes of individual final rises is $\Delta\tilde{h}_f$, defined as

$$\Delta\tilde{h}_f = (\Delta h_{Mf}^3 + \Delta h_{Bf}^3)^{1/3} \tag{D33}$$

What makes (D30) exact while (D33) is only an aproximation? The answer is that in the actual combined plume there is a single time to final rise t_f that applies to both the momentum and buoyancy components. In contrast the individual plumes in the approximation of (D33) each have their own final rise times $\tilde{t}_{Mf}$ and $\tilde{t}_{Bf}$. The approximation lies in adding events that occur at two different times using a sum of cubes law that is really only valid for superposition of effects at the same time of travel.

To find the ratio the exact combined rise in (D30) to the approximate rise in (D33) we first factor out the momentum rise components to write

$$\frac{\Delta h_f}{\Delta \tilde{h}_f} = \left[\frac{\Delta h_{Mf}}{\Delta \tilde{h}_{Mf}}\right] \frac{\left[1 + \left[\frac{\Delta h_{Bf}}{\Delta h_{Mf}}\right]^3\right]^{1/3}}{\left[1 + \left[\frac{\Delta \tilde{h}_{Bf}}{\Delta \tilde{h}_{Mf}}\right]^3\right]^{1/3}} \tag{D34}$$

This ratio will depend on the way in which the atmospheric turbulence dissipation ε varies with height. Using the definitions of the rise components in (D16), (D17) and (D31) and (D32) leads, after some algebraic manipulation, to the final forms

$$\frac{\Delta h_f}{\Delta \tilde{h}_f} = \frac{\left[1 + \frac{\xi}{2} r_1\right]^{3/7}}{\left[1 + \xi^3\right]^{1/3}} \qquad \text{for } \varepsilon \equiv \text{constant} \tag{D35}$$

where ξ and r_1 are defined by (D23), (D24), (D25) and (D26) for constant ε. This constant value of ε is a reasonable approximation for high stacks or for convective turbulence.

For the other limiting case of a ground level release into mechanical turbulence, (D34) and the definitions of the rise components lead to

$$\frac{\Delta h_f}{\Delta \tilde{h}_f} = \frac{\left[1 + \frac{\xi}{2} r_2\right]^{1/2}}{\left[1 + \xi^3\right]^{1/3}} \qquad \text{for } \varepsilon \propto (\Delta h)^{-1} \tag{D36}$$

where ξ and the time ratio r_2 are defined by (D23), (D27), (D28) and (D29) for release into turbulence dissipation ε that varies as $(\Delta h)^{-1}$.

REFERENCES

Batchelor, G.K. and Townsend, A.A. (1956) Turbulent Diffusion, Surveys in Mechanics G.K. Batchelor and R.M. Davies (eds.) Cambridge University Press, p. 352.

Batchelor, G.K. (1952) "Diffusion in a Field of Homogeneous Turbulence II the elative Motion of Particles" Proc. Cambridge Phil. Soc. 48 p. 345.

Benjamin, S.F. (1975) "The Behavior of Hot Plumes from Tall Chimneys Under Conditions of Strong Thermal Convection" Proc. APCA/PNWIS Annual Meeting, Vancouver, B.C.

Bosanquet, C.H. (1957) "The Rise of a Hot Waste Gas Plume" Journal Inst. Fuel, 30, 322-328.

Bosanquet, C.H., Carey, W.F. and Halton, E.M. (1950) "Dust Deposition From Chimney Stacks" Proc. Inst. Mech. Engrs. (London), 162, pp. 355-368.

Briggs, G.A. (1975) "Plume Rise Predictions" in Lectures on Air Pollution and Environmental Impact Analyses, American Meteorological society, Boston, pp. 59-111.

Briggs, G.A. (1969) Plume Rise U.S. Atomic Energy Commission Critical Review Series, Document TID-25075, Clearinghouse for Federal Scientific and Technical Information.

Corsin, S. (1963) "Estimation of the Relation Between Eulerian and Lagrangian Scales in Large Reynolds Number Turbulence" Journal of Atmospheric Sciences 20 p. 115.

Crow, S.C. and Champagne, F.H. (1971) "Orderly Structure in Jet Turbulence" Journal of Fluid Mechanics, 48 part 3, pp. 547-591.

Csanady, G.T. (1973) Turbulent Diffusion in the Environment Reidel, Dordrecht, Holland.

Fackrell, J.E. and Robins, A.G. (1982a) "Concentration Fluctuations and Fluxes in Plumes from Point Sources in a Turbulent Boundary Layer" Journal of Fluid Mechanics 117 pp. 1-26.

Fackrell, J.E. and Robins, A.G. (1982b) "The Effects of Source Size on Concentration Fluctuations in Plumes" Boundary Layer Meteorology 22 pp. 335-350.

Fackrell, J.E. and Robins, A.G. (1981) "Dispersion of Releases at an AGR Site", Central Electricity Generating Board Marchwood Engineering Labs. Report RD/,/1172 R81.

Gifford, F.A. (1982) "Horizontal Diffusion in the Atmosphere: A Lagrangian-Dynamical Theory" Atmospheric Environment 16 pp. 505-512.

Gifford, F. (1977) "Tropospheric Relative Diffusion Observations" Jour. Applied Meteorology 16 pp. 311-313.

Hanna, S.R. (1984) "The Exponential PDF and Concentration Fluctuations in Smoke Plumes", Boundary Layer Meteorology (in press).

Hanna, S.R. (1981) "Lagrangian and Eulerian Time-Scale Relations in the Daytime Boundary Layer" Journal Applied Meteorology 20 pp. 242-249.

Hinze, J.O. (1975) Turbulence 2nd edition, McGraw Hill, New York.

Lee, J.T. and Stone, G.L. (1983) "The Use of Eulerian Initial Conditions in a

Lewellen, W.S. and Sykes, R.I. (1983) "On the Use of Concentration Variance Predictions as a Measure of Natural Uncertainty in Observed Concentration Samples" Proc. Am. Met. Soc. Sixth Symposium on Turbulence and Diffusion, Boston, March 22-25.

Nappo, C.J. (1984) "Turbulence Parameters Derived from Smoke-Plume Photoanlysis" Atmospheric Environment 18, pp. 299-306.

Netterville, D.D.J. (1983) "Plume Rise in Turbulent Winds" Syncrude Environmental Research Monograph.

Pasquill, F. (1974) Atmospheric Diffusion, 2nd ed. Halsted Press (John Wiley and Sons) New York.

Priestly, C.H.B. (1956) "A Working Theory of the Bent-Over Plume of Hot Gas" Quarterly Journal Royal Meteorological Society, 82, pp. 165-176.

Richardson, L.F. (1926) "Atmospheric Diffusion Shown on a Distance-Neighbor Graph" Proc. Royal. Soc. A, 110, p. 709.

Ricou, F.P. and Spalding, D.B. (1961) "Measurements of Entrainment by Axisymmetrical Jets" Journal Fluid Mechanics 11 pp. 21-32.

Robins, A.G. (1984) private communication.

Robins, A.G. (1979) "The Development and Structure of Simulated Neutrally Stable Stable Boundary Layers" Journal Industrial Aerodynamics 4 pp. 71-100.

Sawford, B.L. (1983a) "The Effect of Gaussian Particle-Pair Distribution Functions in the Statistical Theory of Concentration Fluctuations", Quarterly Journal Royal Met. Society, 109, pp. 339-354.

Sawford, B.L. (1983b) "A Lagrangian Statistical Model of Turbulent Concentration Fluctuations", Proc. 8th Australasian Fluid Mechanics Conference, Newcastle Australia, Nov. 28-Dec. 2, 1983. Univ. of Newcastle Printery.

Scorer, R.S. (1959) "The Behavior of Chimney Plumes" International Journal Air Pollution, 1, pp. 198-220.

Slawson, P.R. and Csanady, G.T. (1971) "The Effect of Atmospheric Conditions on Plume Rise" Journal Fluid Mechanics 47(1) p. 33-40.

Slawson, P.R. and Csanady, G.T. (1967) "On the Mean Path of Buoyant, Bent-Over Chimney Plumes" Journal Fluid Mechanics 28, pp. 311-322.

Smith, F.B. (1968) "Conditioned Particle Motion in a Homogeneous Turbulent Field" Atmospheric Environment 2 pp. 491-508.

Snyder, W.H. (1984) private communication.

Snyder, W.H. and Lumley, J.L. (1971) "Some Measurements of Particle Velocity Autocorrelation Functions in a Turbulent Flow" Journal Fluid Mechanics 48 part 1, pp. 41-71.

Spillane, K.T. (1983) "Observations of Plume Trajectories in the Initial Momentum Influence Phase and Parameterization of Entrainment" Atmospheric Environment 17 pp. 1207-1214.

Sykes, R.I., Lewellen, W.S. and Parker, S.F. (1984) "A Turbulent-Transport Model for Concentration Fluctuations and Fluxes" Jour. Fluid Mechanics, 139 pp. 193-218.

Taylor, G.I. (1921) "Diffusion by Continuous Movements" Proc. London Math. Soc., Series 2, 20 pp. 212.

Turner, J.S. (1963) "The Motion of Buoyant Elements in Turbulent Surroundings" Journal of Fluid Mechanics, 16, p. 1.

Wilson, D.J., Robins, A.G. and Fackrell, J.E. (1985) "Intermittency and Conditionally-Averaged Concentration Fluctuation Statistics in Plumes", Atmospheric Environment (in press).

Wilson, D.J. and Simms, B.W. (1985) "Exposure Time Effects on Concentration Fluctuations in Plumes" Alberta Environment Pollution Control Division Technical Report, pp. 4-13.

Wilson, D.J. (1982) "Predicting Risk of Exposure to Peak Concentrations in Fluctuating Plumes", Alberta Environment Report, 90 pp.

Wilson, D.J. (1981a) "Along-Wind Diffusion of Source Transients", Atmospheric Environment, 15, pp. 489-495.

Wilson, D.J. (1981b) "Expansion and Plume Rise of Gas Jets from High Pressure Pipeline Ruptures" Alberta Environment, Pollution Control Division Report, April 1981, 61 pp.

Wilson, D.J. (1979) "The Release and Dispersion of Gas from Pipeline Ruptures", Alberta Environment Pollution Control Division Technical Report, pp. 4-13.